Recent experiments in quantum optics and their implications – II

Amitabh Joshi[†,*] and Suresh V. Lawande[#]

[†]Laser and Plasma Technology Division, Bhabha Atomic Research Centre, Trombay, Mumbai 400 085, India
[#]Department of Physics, University of Pune, Pune 411 007, India

A major thrust in the atomic, molecular and optical physics experiments is mainly on the coherent manipulation of quantum states and research relating to quantum information processing and quantum computation. These themes are manifested in a number of major quantum optical topics such as observation of quantum jumps in ion/atom traps, Bose–Einstein condensation and atom laser, quantum Zeno effect (all these topics have already been discussed in part I of this article), cavity quantum electrodynamics, quantum state engineering, generation of Schrödinger cat states, atom interferometry, wave-packet dynamics, quantum non-demolition measurements, etc. In this article we will be discussing some novel experiments related to these areas.

QUANTUM optics, based on the quantum theory of atomic systems as well as electromagnetic field has come out with many novel physical proposals over the years. There is now a proliferation of experimental techniques that makes it possible to probe the interpretation of quantum theory via ingeneous quantum optics experiments. The present review is devoted to the discussion of these novel quantum optics experiments and their applications. The first part of this article has dealt with experiments on quantum jumps, quantum Zeno effect and interaction-free experiments[1]. In the second part of the article, we will discuss experiments mainly related to cavity quantum electrodynamics (QED). Currently, the major thrust of research in this area is to develop the necessary tools required to realize a quantum network or quantum internet, by employing atom–cavity systems linked by high-fidelity optical interconnects. Photons, when interacting with atoms in small cavities, show a behaviour that is completely unlike that in free space. The interaction between an excited atom and a cavity demands both classical as well as quantum physics to operate simultaneously. Light emission by the atom bridges these two aspects of physics, as the light can be seen as a wave (classically) or as a particle (photon). Also, devices have been created in which spontaneous emission can be halted, accelerated or even completely reversed. A group at Caltech is using optical cavities, where mirrors are separated by 1 mm distance and the reflectivity of these tiny mirrors is about 99.996%. This group has recently observed 'mode-splitting' in an atom–cavity system; we will discuss about this in detail later in the article. The development of superconducting niobium-microwave cavities at Max-Planck Institute of Quantum Optics, Garching has made it possible to operate a 'micromaser' containing only one Rydberg atom. These cavities have also helped in quantum engineering of the 'trapping states' and the 'Fock states' of the electromagnetic field. Questions pertaining to 'which-way' and 'quantum eraser' are also addressed by these cavity QED experiments. The proposed experiments of quantum non-demolition (QND) measurements of photon number are expected to be realized in these high-Q cavities and will be discussed subsequently. Experiments related to the formation of 'Schrödinger cat' will also be discussed. Recent progress towards the trapping of a single atom within a cavity by a single photon will be elaborated. A very recent experiment addressing the issue of wave–particle duality of non-classical light will be described.

*For correspondence. (e-mail: a_joshi@apsara.barc.ernet.in)

Quantum optics in the cavities

Quantum electrodynamics

In a seminal paper in 1927, Dirac quantized the electromagnetic (em) field and obtained the transition rate from spontaneous emission from 'first principles'[2]. This marked the beginning of QED and quantum field theory. It was shown that quantum theory could deal with the actual creation of a particle like the photon in this case. Subsequently, QED was fully developed by Schwinger, Tomonaga and Feynman and became a paradigm of all field theories. Basic issues here involve matter fields where quanta are fermions interacting with force fields whose quanta are bosons. From this point of view, the interaction of a fermion with a boson is one of the most fundamental systems of modern physics.

A primer of basic processes in QED is indicated in terms of Feynman diagrams[2] in Figure 1. QED is concerned with the description of evolution of charged particles coupled to em fields in terms of elementary

processes in which photons are emitted or absorbed. Figure 1 *a* represents spontaneous emission. The photons are created *ex nihilo* (from vacuum). Figure 1 *b* indicates virtual emission of a photon. An electron emits a photon as it is perturbed by the vacuum and shortly thereafter, this photon is absorbed. The electron is surrounded by a cloud of virtual photons which slightly change their mass and shift their energy levels. This is related to the self-energy of the free electron in which the electron is considered to be in the positive part of the Dirac's equation for a free particle. Figure 1 *c* shows the binding of atoms and molecules in solids, which involves an exchange of a photon between a proton and an electron (equivalent of Coulomb interaction). Figure 1 *d* indicates spontaneous emission in an atom. The electron and the proton are bound together with the electron undergoing a quantum jump by spontaneously emitting a photon[2].

Each diagram is a possible history for an interacting charge-field system. QED assigns a complex number amplitude to each history. The probability of a process with a given initial state and a given final state is the absolute square of the sum of the amplitudes corresponding to all possible intermediate photon and particle states. Due to the wave nature of photons and particles, interference is expected. At low energies, particles are conserved but photons can be created or destroyed. The lowest state of the radiation is vacuum and photons can be created from vacuum. In this state em fields have non-vanishing fluctuations. This is a consequence of the relation $[a, a^\dagger] = 1$ (non-commutation of a and $a^\dagger$). The radiation field is similar to a collection of harmonic oscillators which have non-vanishing 'zero-point' energy even in their ground state.

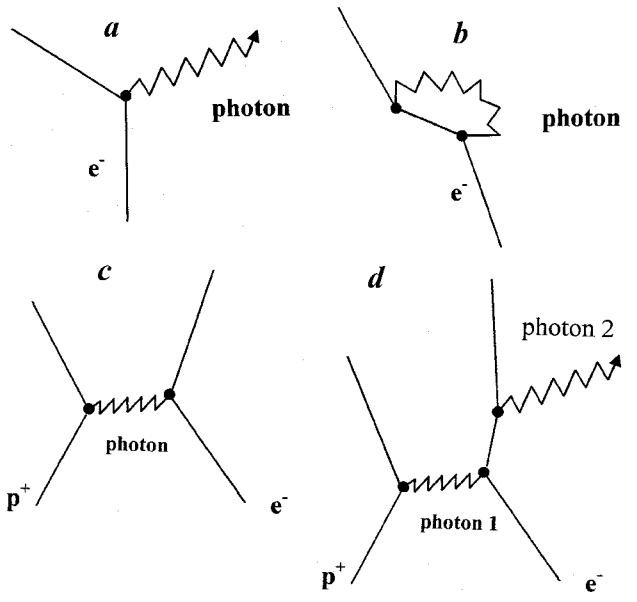

Figure 1. Elementary QED processes as described by Feynman diagrams. ***a***, Spontaneous emission process in which a photon is emitted when an electron jumps between its quantum states; ***b***, Electron emits a photon whose energy is different from the electron transition energy and quickly reabsorbs this photon. So the electron is surrounded by a cloud of virtual photons; ***c***, Interaction between a proton and an electron by exchange of a photon; ***d***, Bound system of an electron and proton in which the electron is undergoing quantum jumps by spontaneously emitting a photon.

Elementary atom–photon interactions are strongly modified when an atom is confined in a cavity. This is because in a cavity of length d, modes with wavelength $\lambda > 2d$ are frozen out. This has prompted experiments for new fundamental tests of quantum theory at very low energies.

The Jaynes–Cummings model

A simple but non-trivial model of interaction of a fermion with a boson was proposed by Jaynes and Cummings in 1963 (ref. 3). The model considers the interaction of a single mode of em field with a single two-level atom. The model has been a useful paradigm for a variety of reasons: (i) It is mathematically tractable and yields exact analytical solutions for arbitrary coupling constants. (ii) It predicts certain 'revival phenomenon' of Rabi oscillations, which is a signature of the quantum nature of the field. (iii) It is sensitive to the quantum statistics of the field. (iv) It exhibits squeezing and shows chaotic behaviour in the semiclassical limits. The model had only academic interest initially. However, the development of tunable lasers allowed study of the highly excited Rydberg states of atoms for three reasons: (i) These states are strongly coupled to the radiation field. The probability of the induced transition between adjacent states is large and scales as n^4. (ii) The transitions to neighbouring levels are in the region of millimeter waves, which permits one to build cavities with large low-order modes to ensure long interaction times. (iii) The Rydberg atoms have long spontaneous emission lifetimes, so that only the coupling with the selected cavity mode is important. In fact, the spontaneous emission lifetime scales as n^3 and n^5 for low and high angular momentum states, respectively. Therefore, the saturation power for the transition between neighbouring states becomes extremely small. The other ingredient of these experiments is the development of low-temperature superconducting cavities with high quality factors. In such cavities, the relaxation time is much larger than the characteristic time of the atom–field interaction. The latter is given by the reciprocal of the Rabi frequency. Thus a periodic exchange of a photon between the atom and the cavity field can be observed.

Basic theory: The JCM considers a single two-level atom, with the ground state $|g\rangle$ and the excited state $|e\rangle$ and transition frequency ω_0, interacting with a quan-

tized single mode of radiation field of frequency ω in a cavity. The Hamiltonian in RWA[3] is given by

$$H = \hbar\omega_0 S_z + \hbar\omega a^\dagger a + \hbar g(S_+ a + S_- a^\dagger), \quad (1)$$

where $S_\pm$ and S_z are the atomic operators.

$$S_+ = |e\rangle\langle g|, \quad S_- = |g\rangle\langle e|, \quad S_z = \tfrac{1}{2}[|e\rangle\langle e| - |g\rangle\langle g|], \quad (2)$$

and $a(a^\dagger)$ is the field annihilation (creation) operator. The Hamiltonian H can be diagonalized easily. The resulting eigenstates $|\psi_n^\pm\rangle$ (dressed states) and the corresponding eigenvalues $\lambda_n^\pm$ are as follows (under resonance $\omega_0 = \omega$, $\hbar = 1$):

$$H|0, g\rangle = -\frac{\omega}{2}|0, g\rangle,$$

$$H|\psi_n^\pm\rangle = \lambda_n^\pm |\psi_n^\pm\rangle,$$

$$\lambda_n^\pm = \omega[(n+1/2) \pm g\sqrt{n+1}],$$

$$\Omega_{n,}^2 = g^2(n+1),$$

$$|\psi_n^\pm\rangle = \frac{[|n, e\rangle \pm |n+1, g\rangle]}{\sqrt{2}}. \quad (3)$$

The quantum electrodynamic calculations of this model proceed from the fully quantum Hamiltonian (eq. (1)). We take the atom initially to be in the excited state $|n\rangle|e\rangle$ which gets coupled to the state $|n+1\rangle|g\rangle$ by the Hamiltonian (eq. (1)). Then the probability of finding the atom in the excited state is

$$P_e(t) = \cos^2(gt\sqrt{(n+1)}), \quad (4)$$

and that in the ground state is

$$P_g(t) = \sin^2(gt\sqrt{(n+1)}). \quad (5)$$

This implies also that the inversion $W(t)$

$$W(t) = 2\langle S_z(t)\rangle = \cos(2gt\sqrt{(n+1)}), \quad (6)$$

and hence

$$\langle a^\dagger(t)a(t)\rangle = \langle N(0)\rangle - \langle S_z(t)\rangle = n + \sin^2(gt\sqrt{(n+1)}). \quad (7)$$

When n 1, we have, $a^\dagger(t)a(t)\rangle \approx n$ and $P_e(t) \approx \cos^2(\Omega t)$, $P_g(t) = \sin^2(\Omega t)$, where $\Omega \sim g\sqrt{n}$ is the Rabi frequency.

In more conventional (semi-classical) terms, $\Omega = dE_0/\hbar$, where d is the transition dipole moment and E_0 is the electric field amplitude (proportional to $\sqrt{n}$). In this limit, the atom is driven by an effectively constant applied field. This is the limit in which semiclassical radiation theory is expected to hold.

The limit $n \to 0$ implies that there is no field, semiclassically. However, when $n \to 0$, the above equations predict that

$$P_e(t) = \cos^2(gt), \quad P_g(t) = \sin^2(gt), \quad (8)$$

$$\langle a^\dagger(t)a(t)\rangle = \sin^2(gt) = P_g(t). \quad (9)$$

These equations describe the vacuum field Rabi oscillations. This is purely a quantum effect describing periodic reversible spontaneous emission! In the normal or classical sense, the spontaneous emission means that the excited state irreversibly decays to the ground state. Here, the field quantization in the cavity has made it possible for the atom to interact with the vacuum of the field or the lowest energy state of the quantized harmonic oscillator (which is not possible classically), and the field oscillates periodically as the single photon is tossed between the excited and the ground states of the atom, describing a periodic reversible spontaneous emission. When the atom is in ground state there is one photon present in the cavity field which is reabsorbed by the atom. After some time the atom is in the excited state and there is no photon in the cavity field.

The results can be further generalized to cases where the initial field state is not one of the definite photon number, but rather a superposition of all such number states.

For a thermal field, the probability of having n photons in the field with mean photon number as $\bar{n}$ is given by $P(n) = (\bar{n})^n/(\bar{n}+1)^{n+1}$. Hence,

$$P_e(t) = (\bar{n}+1)^{-1}\sum_{n=0}^{\infty}\left(\frac{\bar{n}}{\bar{n}+1}\right)^n \cos^2(gt\sqrt{(n+1)}). \quad (10)$$

For the case when the atom is in the upper state at $t = 0$, thermal occupation of resonant cavity modes is important. The behaviour is chaotic (Figure 2).

Consider the case when the field in the cavity is in a coherent state $|\alpha\rangle$ with mean photon number $|\alpha|^2 = \bar{n}$ and photon distribution $P(n) = (\bar{n})^n e^{-\bar{n}}/n!$. Here the excitation probability is given by

$$P_e(t) = \sum_{n=0}^{\infty}(\bar{n}^n/n!)e^{-\bar{n}}\cos^2(g\sqrt{(n+1)t})$$

$$= \frac{1}{2}\left[1 + \sum_{n=0}^{\infty}(\bar{n}^n/n!)e^{-n}\cos(2gt\sqrt{(n+1)})\right]. \quad (11)$$

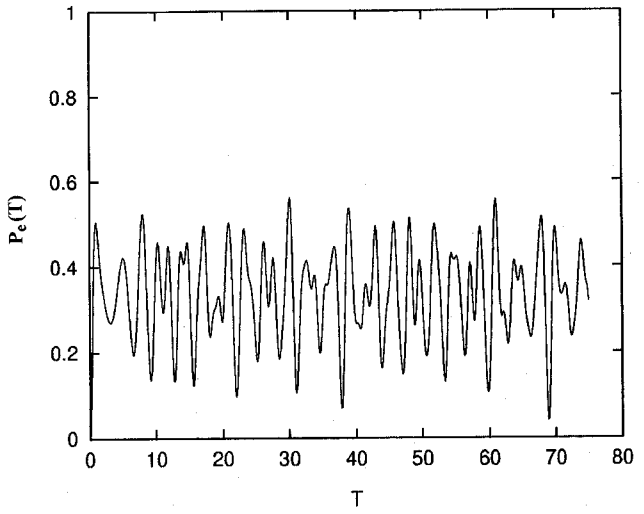

Figure 2. Atomic excitation probability as a function of time for a two-level atom undergoing one photon transition in an ideal cavity with thermal field of mean photon number $\bar{n} = 10$.

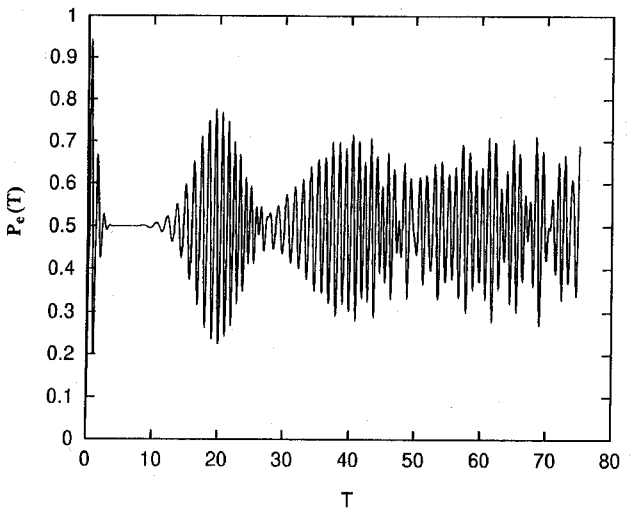

Figure 3. Same as Figure 2, but for the coherent field of mean photon number $\bar{n} = 10$.

An atom interacting with a coherent state field sees a spread in field strength and a spread in Rabi frequencies. This gives rise to collapses and revivals of Rabi oscillations (Figure 3). Spread in Rabi frequencies leads to dephasing of Rabi oscillations, as was pointed out by Cummings[4]. The dephasing time

$$T_c^{-1} = \frac{1}{\Delta n}\left[g(\bar{n}+\Delta n)^{1/2} - g(\bar{n}-\Delta n)^{1/2}\right] \simeq g, \tag{12}$$

which is independent of $\bar{n}$. Oscillations are damped with a Gaussian envelope. For longer times, the system exhibits a series of revivals and collapses. The revival time

$$t_r = \frac{2\pi\sqrt{\bar{n}}}{g}. \tag{13}$$

Revivals are due to grainy nature of the field. The atomic evolution is determined by the individual quanta[5].

Let us surmise the basic reasons for the revivals. A single-mode quantized em field is expressed as the operator

$$\hat{E} = iE_0(a e^{-i(\omega t - k.r)} - a^\dagger e^{i(\omega t - k.r)}), \tag{14}$$

$$E_0 = \left[\frac{\hbar\omega}{2\varepsilon_0 V}\right]^{1/2}. \tag{15}$$

The expectation values of the field $\hat{E}$ and $\hat{E}^2$ in a Fock state $|n\rangle$ are given by

$$\langle n|\hat{E}|n\rangle = 0, \ \langle n|\hat{E}^2|n\rangle = E_0^2(2n+1). \tag{16}$$

Even when $n = 0$, $\langle 0|\hat{E}|0\rangle = 0$, but $\langle 0|\hat{E}^2|0\rangle = E_0^2 \neq 0$. This is due to vacuum fluctuations.

Now consider the coherent state $\hat{a}|\alpha\rangle = \alpha|\alpha\rangle$.

$$|\alpha\rangle = e^{-|\alpha|^2/2}\sum_{n=0}^{\infty}\frac{\alpha^n}{\sqrt{n}}|n\rangle, \ \alpha = |\alpha| e^{i\phi}. \tag{17}$$

The expectation values of $\hat{E}$ and $\hat{E}^2$ in the coherent state $|\alpha\rangle$ read as

$$\langle\alpha|\hat{E}|\alpha\rangle = -2E_0|\alpha|\sin(\vec{k}.\vec{r} - \omega t + \phi), \tag{18}$$

$$\langle\alpha|\hat{E}^2|\alpha\rangle = E_0^2(4|\alpha|^2 \sin^2(\vec{k}.\vec{r} - \omega t + \phi) + 1), \tag{19}$$

$$(\Delta E)^2 = \langle\alpha|\hat{E}^2|\alpha\rangle - (\langle\alpha|\hat{E}|\alpha\rangle)^2 = E_0^2. \tag{20}$$

Thus, a coherent state of the field is equivalent to a classical field plus vacuum fluctuations. This means that when the cavity field is in a coherent state $|\alpha\rangle$, the effective Hamiltonian is

$$H = \hbar\omega(S_z + a^\dagger a) + \hbar g[S_+(a + \alpha) + (a^\dagger + \alpha^*)S_-]. \tag{21}$$

In this picture, the initial state is the ground state atom and the vacuum cavity field state. The coherent field excites the atom from the lower state $|g, n\rangle$ to the upper state $|e, n\rangle$ without changing the photon number n. However, the excited atom decays from $|e, n\rangle$ to the ground state $|g, n+1\rangle$ by virtue of the JCM coupling. Thus the collapses and revivals are a consequence of the 'grainy' nature of the field which introduces quantum 'leakage'

correction to the sinusoidal Rabi oscillations predicted classically. If we replace the right hand side of the eq. (11) by a semiclassical expression, but assume that atom initially be in its ground state than we have

$$P_e(t) = \frac{1}{2}\left[1 - \sum_{n=0}^{\infty} P(n)\cos(2gt\sqrt{(n+1)}\right] = \frac{1}{2}\left[1 - \int_0^{\infty} P(I)\cos(2gt\sqrt{I})\mathrm{d}I\right], \quad (22)$$

where $P(I) = e^{-I/\langle I\rangle}/\langle I\rangle$. The resultant expression is

$$P_e^{sc}(t) = \theta D(\theta), \quad (23)$$

in which $\theta = \langle I\rangle^{1/2} gt$ and $D(\theta)$ is Dawson's Integral:

$$D(\theta) = e^{-\theta^2}\int_0^{\theta} e^{x^2}\mathrm{d}x. \quad (24)$$

The excitation probability shows a single collapse and no revivals, thereby indicating that the revival is a signature of the quantum nature of the field (Figure 4).

Note also that in the case of an initial thermal state, the collapses and revivals are present but much less distinct. This is because of the much broader distribution of photon number in this case compared to the coherent case[6]. Many interesting effects in JCM arising due to atom–field coupling coefficient have been discussed recently[6].

Experimental observations

Evidence for collapse and revival in the JCM has been observed in some extraordinary experiments at MPQ, Garching near Munich[7], with Rydberg atoms in high-Q cavities. In these experiments a velocity-selected beam of Rb atoms was excited by ring-dye laser systems to the $^{63}P_{3/2}$ Rydberg state and then the atoms passed through a superconducting microwave cavity operating on a single-mode frequency of 21.6 GHz near the $^{63}P_{3/2} \rightarrow {}^{61}D_{5/2}$ transition frequency. The cavity was cooled to 0.5 K, so that the mean thermal photon number $\bar{n} = 2$ and the photon decay time in the cavity is sufficiently large (2 ms) that an atom could interact with the spontaneously emitted photon. The atomic beam flux was so low (500–3000 atoms per second) that only a single atom at a time was present in the cavity, and the cavity field could relax back to the equilibrium between passage of successive atoms. Thus, the experiment was designed to simulate JCM with an initial thermal state of mean photon number $\bar{n} \approx 2$.

Atoms exiting the cavity were detected via field ionization with a field strength such that $^{63}P_{3/2}$ atoms were ionized. The interaction time of an atom with the field was varied by selecting different atomic velocities and the probability of detection is reconstructed as a function of interaction times. The use of larger flux of atoms than the $500\ s^{-1}$ increased the cavity photon number. Evidence of both collapse and revival of Rabi oscillations was seen and the data are consistent with theoretical analysis and prediction of JCM.

One-atom maser

The one-atom maser or the micromaser is physically a very tiny device in which atoms are radiating in a high-Q cavity one by one and the field so generated is 'non-classical'. This is one practical example where concepts of cavity QED are directly applicable. Experimental techniques with Rydberg atoms, similar to those used to study the JCM have been applied to the development of a 'one-atom maser'[8] (see Figure 5). The basic idea of these experiments is to pass atoms through a cavity fast enough compared with photon decay rate, that a photon

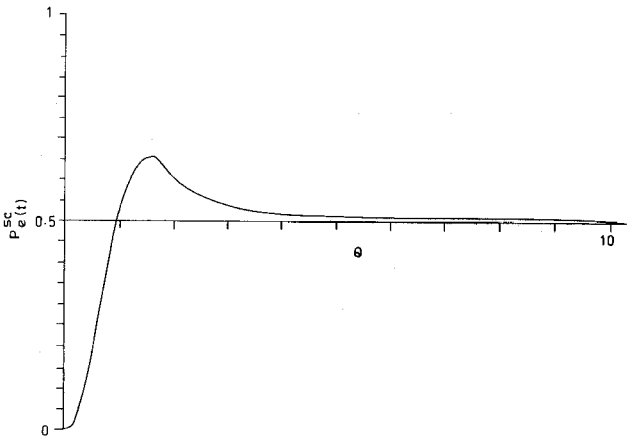

Figure 4. Time evolution of the inversion of two-level atom driven by classical chaotic field vs $\theta = \langle I\rangle^{1/2} gt$.

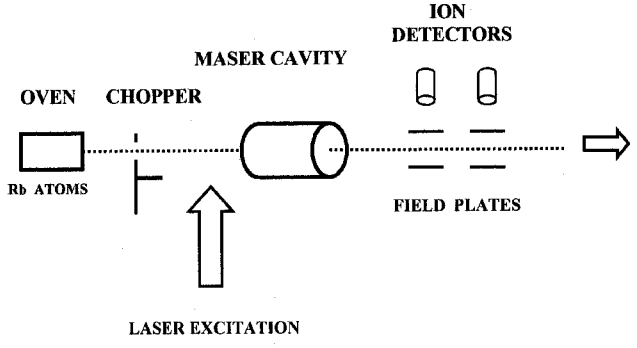

Figure 5. Schematic diagram of one-atom maser or micromaser.

emitted by an atom remains in the cavity long enough to interact with the next atom. Then the cavity photon number can grow by stimulated emission. Maser action with atomic beam flux as low as $100\ s^{-1}$, with an average of only 0.06 atom in the cavity at a time has been achieved in this way. The atoms in a sense 'kick' the field mode as they pass through the cavity[9].

It has also been possible to construct a two-photon micromaser using an Rb atomic beam excited to the $40S_{1/2}$ state[10]. The beam passed through a superconducting cavity tuned to half the $40S_{1/2}$–$39S_{1/2}$ transition frequency. At this frequency, tuning the $40S_{1/2}$–$39P_{3/2}$ (one photon) spontaneous emission is suppressed so that two-photon transition becomes the dominant radiative channel. The two-photon process in the cavity is discussed later in the article.

Vacuum Rabi splitting

Another interesting area of cavity QED deals with dispersive effects and the radiative shifts of atomic energy levels due to the cavity and also the corresponding shifts of frequency of the cavity containing several atoms[11]. If the strength of atom field coupling is more than the system dissipation rate, then it is called the strong coupling cavity QED regime[11]. Under strong coupling conditions, nonlinear effects such as Rabi oscillations of atomic population and the dynamical splitting of the system resonance lines are expected. These effects have to be dealt by non-perturbative methods, even if the field is in the vacuum state[11–13]. The atom–em field mode coupling parameter is $\Omega(\vec{r}) = E_0(\vec{r})p/\hbar$, where $E_0(\vec{r}) = f(\vec{r})(\hbar\omega/2\varepsilon_0 V)^{1/2}$. It is called rms (root mean square) amplitude of vacuum field in the mode at the vector coordinate $\vec{r}$. The dipole operator matrix element connecting the ground state $|g\rangle$ to the excited state $|e\rangle$ is defined by p, $f(\vec{r})$ is related to the spatial distribution of the mode and the effective cavity volume is V. For the strong cavity coupling condition $\Omega \geq \gamma, \kappa$ (γ, κ are radiative and cavity damping coefficients, respectively) must be satisfied. This has been achieved in two different kinds of experiments. For the experiments in optical wavelength region, advancement in the technology to fabricate small-sized mirrors has made it possible to construct millimeter-size Fabry–Perot cavities of very high finesse and enclosing large vacuum fields. In such cavities, experiments have been performed using alkali or alkaline earth resonant lines and Ω, γ, κ are found to be of comparable magnitude ($\sim 10^6$ to $10^7\ s^{-1}$). In yet another set of experiments, E_0 is much weaker as ω is smaller and V is larger. However, this drawback can be overcome by coupling the cavity to a Rydberg transition. The Rydberg atom intrinsically possesses a large electric dipole transition matrix element. The coefficient γ is small in Rydberg atoms and κ can be made smaller by using superconducting cavities cooled down to 0.5–2.0 K. Typical values of Ω, γ, κ are in the region $\sim 10^6$, 1, $10^5\ s^{-1}$, depending upon the atomic transition and other parameters of the cavity.

The dressed states introduced earlier can be conveniently used for analysing radiative shifts in non-perturbative cavity QED regime. We consider a system consisting of a single two-level atom and a photon (of the cavity mode) which can drive it. The ground state of this system is $|g, 0\rangle$ meaning thereby that the atom is in its lower state and the field in the vacuum state. The lowest excited states of the system are $|e, 0\rangle$ and $|g, 1\rangle$: meaning that the atom is in the upper state and the field in the vacuum state, and that the atom is in the lower state with a photon in a mode. These uncoupled states are separated by an amount $\Delta = \omega - \omega_g$ which is called cavity–atom detuning. However, at resonance, viz. $\Delta = 0$, the states $|e, 0\rangle$ and $|g, 1\rangle$ are degenerate in energy. The degeneracy is lifted once the atom–field coupling $\Omega(\vec{r})$ is switched on. We get two dressed states which are a linear combination of these states $|e, 0\rangle$ and $|g, 1\rangle$. Specifically, the two dressed states are $|\pm\rangle = \cos(\theta)\ (-\sin(\theta))|e, 0\rangle + \sin(\theta)(\cos(\theta))|g, 1\rangle$ with $\tan(2\theta) = -2\Omega/\delta$ $(0 < \theta < \pi/2)$. This manifold is shown in Figure 6 (inset). At resonance the splitting in the manifold is $2\Omega(\vec{r})$. When this system of atom–cavity is probed with a weak field whose frequency ν is being swept across, then the probe can resonantly couple energy into the atom–cavity system only when its frequency exactly matches with one of the dressed-state frequencies. At exact resonance, $\omega = \omega_g$ also, the probe beam does not get absorbed at $\nu = \omega$ but there is absorption at $\nu_\pm = \omega \pm \Omega$. This spectrum is called dynamical vacuum Rabi splitting spectrum (Figure 6)[11–13]. This splitting spectrum is similar to the dynamical Stark

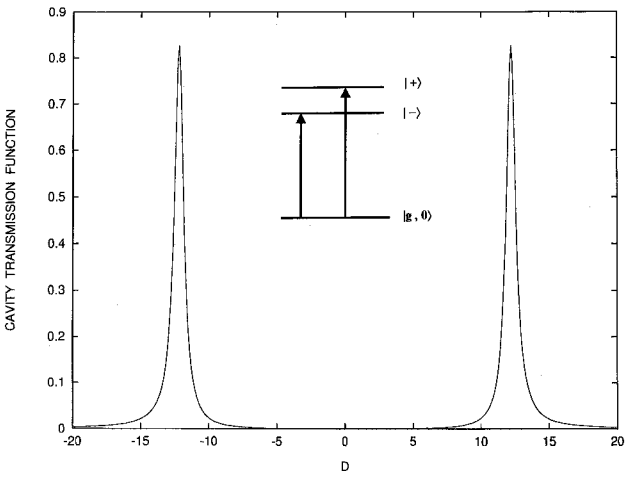

Figure 6. Vacuum Rabi splitting observed on the Fabry–Perot cavity transmission spectrum (here, $D = \nu - \omega_g$). The cavity is filled with atomic vapours. (Inset) Ground state and first two dressed (atom–cavity) states. The two transitions probed by a weak field constitute vacuum Rabi splitting.

splitting spectrum seen in optical and microwave resonance of the atoms. The cavity resonance splitting also reminds us of the cavity frequency pulling effect which occurs when a macroscopic medium, whose refractive index is different from unity, is placed inside the mode.

The experiments usually performed to observe vacuum Rabi splitting effects involve a large number of identical Na atoms coupled to a high-Q cavity mode. The lowest state of the system is the product state $|L\rangle = |g\rangle|g\rangle\ldots|g\rangle\ldots$, which means all the atoms are in their lower levels $|g\rangle$. A weak excitation by a single photon brings the atomic system in a collective state $|H\rangle$ in which energy is evenly shared by the atoms. The dipole matrix between these states is equal to $p(N_a)^{1/2}$. This collective atomic system is more strongly coupled to the cavity than the single atom. So, the weak excitation spectrum of the cavity, when probed by a weak field, consists of two lines whose separation under resonance condition ($\Delta = 0$) is given by $2\Omega_{av}(N_a)^{1/2}$ in which Ω_{av} is average coupling (averaged over the spatial extent of the atom). In the optical regime, the vacuum Rabi splitting has been observed on the transmission spectrum of a small Fabry–Perot cavity crossed by sodium or barium atomic beam with $N_a = 300$ atoms[11]. The minimum number of atoms giving rise to an observable splitting is approximately 30. These experiments, when performed in microwave regime using superconducting microwave cavity, show a vacuum Rabi splitting with about 10 atoms[11]. The experiments, performed by Mossberg's group[11] for investigating vacuum Rabi splitting in optical regime, utilizes both continuous wave input as well as pulsed input. Besides this, they have also shown that their results are in excellent agreement with a 'completely classical model'. The 'classical model' involves calculation of cavity transmission function from the standard theory of multibeam interferometery applied to the Fabry–Perot cavity containing atoms with linear absorption and dispersion[11].

Complimentarity in quantum mechanics

In quantum mechanics, the question of 'complimentarity' is intriguing[14]. In certain physical processes, matter exhibits particle-like properties, but in other processes, it displays wave-like properties and gives rise to interference phenomenon of matter waves. The Welcher–Weg (German word for 'which path') information essentially comes from the particle nature of matter or light. Young's double-slit experiment[15] has demonstrated the wave–particle duality in a convincing manner. In this experiment, while observing the interference pattern on the screen it is not possible to predict from which slit the light has come from. If we make an attempt to find out 'which path' information then the interference pattern will disappear. Einstein tried to modify this experiment by using recoiling slits so that we can simultaneously observe an interference pattern as well as get the 'which path' information. However, this proposal was found to be deceptive in the sense that the position of recoiling slits is known within some uncertainty governed by the uncertainty principle. Consequently, a random phase will be imparted to the light beams and hence interference pattern washes out[15].

Welcher-Weg detection: A Welcher-Weg detection experiment analogous to Young's double slit experiment has been proposed by the Munich group utilizing two consecutive micromasers[16]. The ^{85}Rb atomic beam in which each atom is in coherent superposition of states $^{63}p_{3/2}$ and $^{63}p_{1/2}$ enters the first micromaser cavity and undergoes a transition $^{63}p_{3/2}$ to $^{61}d_{5/2}$ in the micromaser cavity (Figure 7). When the atom enters the second micromaser cavity, it undergoes another transition $^{63}p_{1/2}$ to $^{61}d_{3/2}$. The control of these transitions in two maser cavities is extremely sensitive to various experimental parameters like atomic velocity, etc. Essentially, the initial atomic coherence (of p-states) is transferred to d-states in this process of crossing two micromaser cavities. This can be observed via field ionization of the atoms in d-states, where the detector current shows up a modulation or quantum beating[16,17]. Whether the ionization current will show modulation or not depends on the nature of the field states set in the microwave cavities. Suppose the micromaser fields are initially in a coherent state with large mean photon number, the emission of two photons, one by one, in the two micromaser cavities will not change the initial field state appreciably. This implies that it will be difficult to know whether the

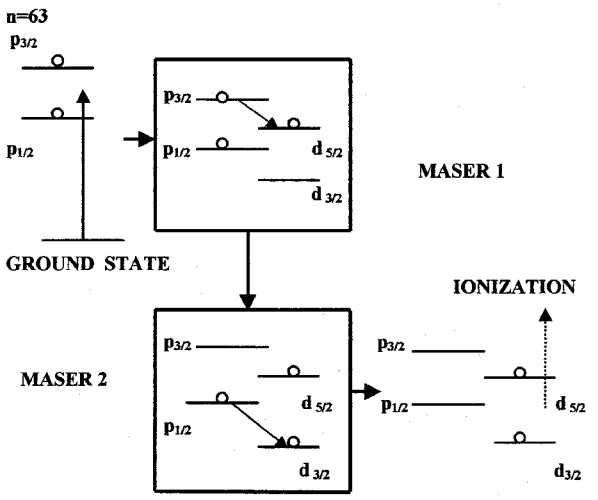

Figure 7. Welcher-Weg detection using micromasers. Rb atom in a coherent superposition of its states $^{63}p_{3/2}$ and $^{63}p_{1/2}$ is moving in maser 1 such that the state $^{63}p_{3/2}$ de-excites to $^{61}d_{5/2}$. When it moves to maser 2, the state $^{63}p_{1/2}$ de-excites to $^{61}d_{3/2}$. Quantum beats in photoionization will or will not be detected depending on the state (coherent or Fock) of the field in the masers.

emission of atoms has taken place or not in the maser cavities and coherence will be preserved, giving rise to the modulation in ionization current. On the contrary, if the micromaser cavities are initially in a Fock state with well-defined photon number, then emission of a photon by the atom will be possible as the photon number will be increased by 1 but, in the process, the coherence will be destroyed and ionization current will not show any modulation[16,17]. The 'Welcher-Weg' information about the emission path of atoms comes when the micromasers are initially in Fock states. Any emission will cause a change of Fock state by one photon. For example, let initially the first micromaser be in the Fock-state $|n_1\rangle$. If after the Rydberg atom passes through it, we come to know that it has become $|n_1 + 1\rangle$ then we know that the emission path of the atom is transition $^{63}p_{3/2}$ to $^{61}d_{5/2}$. Similarly, if we have a knowledge about the Fock state of the second micromaser cavity after the atom has passed through it, then clearly the atomic emission path is $^{63}p_{1/2}$ to $^{61}d_{3/2}$. Thus we can now draw an analogy of the micromaser experiments with the Young's double-slit experiment. Here the role of recoiling slits (that provide information on emission path) is being played by the photon states of the micromaser cavity.

As we have discussed above, the 'which-way' detector suggested by Einstein in the Young's double-slit interference experiment does not work because it is inconsistent with the uncertainty relation. However, another question under debate has been whether Heisenberg's uncertainty relation is more fundamental or the Bohr's principle of complimentarity! Usually, it is presumed that the uncertainty relation enforces complimentarity, but this is not always the case because in a recent thought-experiment, a possibility to construct a 'which-way' detector that does not affect the motion of the observed object, has been clearly brought out. In other words, the possible experiment of 'which-way' detectors that will get around the uncertainty relation has been clearly proposed.

Conceptually, this experiment is a variant of the double-slit experiment interferometer along with Feynman's proposal[18]. Feynman, in his proposal for 'which-way' information experiment, suggested to replace photons by electrons in the usual double-slit experiment. As the electrons are charged particles, they can interact with the em field or the photon field. Feynman suggested to put a source of photon symmetrically between the two slits. If the photon collides with the electron, then it will be scattered. The direction of scattering will precisely determine the slit it has originated from. In this experiment, the momentum imparted to the electron and the uncertainty in the position are both important parameters. These parameters should be very small (than those allowed by Heisenberg's uncertainty relation) in order to have interference as well as 'which-way' information.

In the proposed new thought-experiment by the Munich group[19,20], electrons are replaced by atoms. The arrangement is as shown in the Figure 8 *a*. Essentially, it is a single-atom experiment using micromaser-like cavities. A laser is used to put collimated atoms into their excited state. Once the atoms move (one by one) to the upper or lower cavities, they are forced to de-excite to a lower state by emitting a longer wavelength photon, giving us 'which-way' information. But one does not get any interference pattern. Perhaps the atoms are labelled by the photons they have left in the cavity. This means that one cannot get around the Bohr's principle of complimentarity, though it is possible to circumvent the Heisenberg's uncertainty relation. In a recent experiment by Haroche's group (see ref. 19), the confirmation of complimentarity has been reported.

Quantum eraser experiment: This is just like the 'which-way' detection type of experiment, but with a

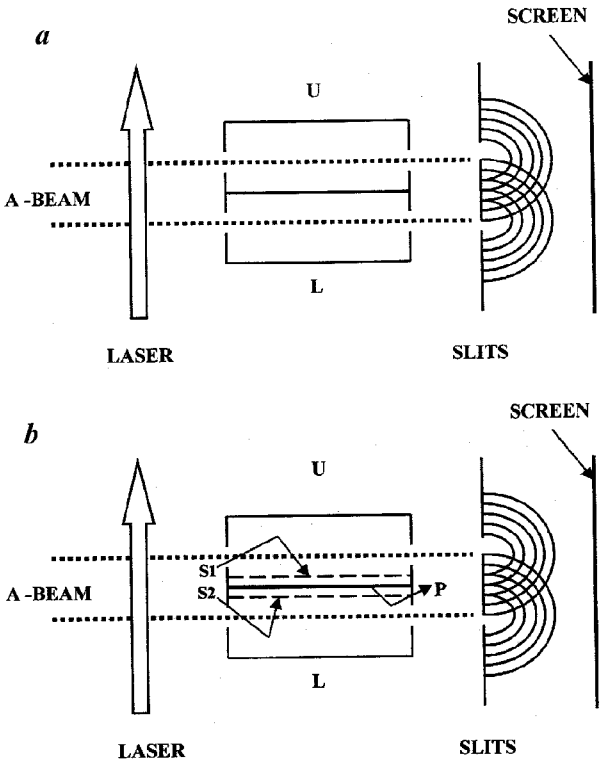

Figure 8. *a*, Collimated atomic beam excited by a laser is moving in such a way that when the atom crosses the upper (U) or the lower (L) cavity, it is de-excited and leaves a photon in that cavity and could be detected. De-excitation of an atom has no effect on the atomic motion, so the uncertainty relation is circumvented. However, the interference pattern (atoms are behaving as waves) is washed out due to 'which-way' information or the photon tagging on the cavity; *b*, Quantum-eraser counterpart of the experiment (*a*). Here S1 and S2 are shutters and P the photosensor. When an atom comes out and hits the screen, both the shutters get open. When the photon gets absorbed by the photosensor, the atom on the screen is marked as *x*, otherwise *y*. The *x* spots make an interference pattern and the *y* spots make a complimentary pattern.

slight variation. The motivation for this experiment is to find the answer for the converse proposal for the complimentarity issue. What we mean by this is to erase the 'which-way' information by allowing the labelling photon to get absorbed within the little box (cavity) and then see whether the interference pattern re-emerges[19]. We first discuss the thought-experiment demonstrating the quantum eraser of 'which-way' information as given by the Munich group[19]. Essentially, the set-up is that shown in Figure 8*b* where a photon detector sits between the cavities and it is covered on both sides by a shutter. When the shutters are closed, we have two different cavities and the situation is similar to the 'which-way' detector as discussed above (Figure 8*a*). Next, in the empty cavities the atom is sent. After crossing the cavities the atom leaves behind a photon in one of the cavities and it reaches the screen and makes a spot. When this is happening, the shutters are simultaneously opened and as a consequence the two cavities are now merged to become a single large cavity. It is quite obvious to assume that now photon will strike the detector. But, something interesting happens at this stage. Initially when the shutters were closed, there were two partial waves associated with the photon in each cavity. After opening the shutters, these two partial waves combine to form a single wave. Suppose the partial waves combine in such a way that they reinforce each other at the photon detector, then one observes a signal. If the partial waves have opposite phase at the photon detector, then no signal will be obtained. One can say that there are equal chances for each event to occur. The positions of the atoms striking the screen can be marked when there is a signal and no signal. These positions will be different in the two cases. The pattern emerging on the screen due to the collection of the atoms can be analysed. An interference pattern emerges (similar to the Young's double-slit experiment) when one collects those positions of atoms from which there were signals in the photon detector, i.e. when the photon is destroyed or erased. The pattern formed by those atomic spots which are obtained when there is no signal in the photon detector (i.e. photon is intact) is just the complimentary of the interference pattern obtained with the photon erased. It is important to note that only by correlating the atoms hitting the screen with the response of the photon detector, the interference patterns are brought back.

Practical realization of the quantum eraser experiment is found to be very difficult as the excited atoms supposed to enter the tiny cavities are very fragile and can be lost very easily. Besides this, there are some technical problems, for example, the release of the photon may cause disruption of the atom's forward momentum. The Innsbruck group[21] resolved this issue by using photons in the experiment rather than atoms as suggested in the thought-experiment by the Munich group. The photon source used in the experiment is an ultraviolet laser photon down-converting itself into two correlated red photons of equal frequency, while nonlinearly interacting with a crystal. In case down-conversion of the photon does not occur while moving in the forward direction, then this photon is reflected back by the mirrors and reallowed to pass through the same crystal so that two photons in pair can be generated. The pair of photons have definite correlation and move in separate directions and eventually get recorded by the detectors. So, there are two ways in which this pair of photons can be generated and thus constitute two objects that interfere (Figure 9). This is because the placement of mirrors and the reflection of the light take place in such a way that it is impossible to know whether photons are created by the forward laser beam or the returned beam. In other words, these two possibilities of generation of photons create two paths corresponding to those of the double-slit experiment, in which a photon can move through. The interference pattern emerges at each detector due to the phase difference between two photons striking at the detectors. This phase difference arises due to slightly different optical paths taken by the photons. Suppose photons arrive in phase at the detector, then it is called as a bright fringe part of the interference pattern. When the photons arrive out of phase, then it corresponds to dark fringe part. The interference pattern can be made to disappear if the photons can be tagged or marked. If one of the photons can be tagged, then it provides 'which-way' information and hence the interference pattern disappears concurring with Bohr's

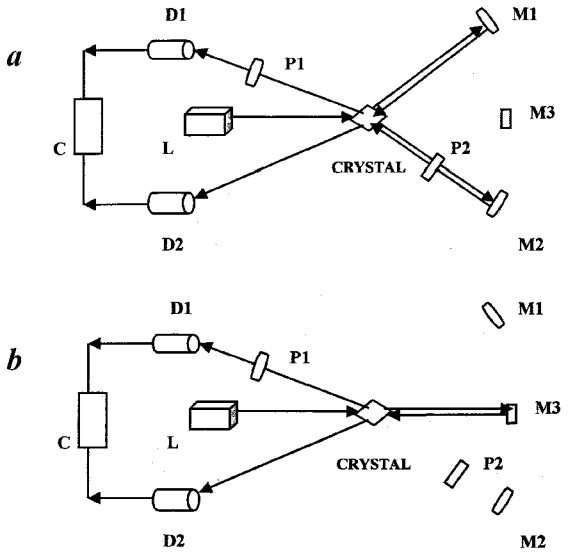

Figure 9. Quantum eraser experiment scheme of Herzog *et al.*[21]. Laser (L) produces two correlated photons from a down-conversion crystal in two ways (***a***) when the laser beam goes through directly; (***b***) or when the reflected laser beam (from M3) passes through the crystal. Polarization rotator P2 gives the 'which-path' information while the polarization rotator P1 erases the information.

complimentarity principle. Tagging to the photon can be provided by giving it a rotation in its polarization so that its momentum is not affected. This kind of tagging can be erased by restoring the polarization of the photon at some other place in the optical path. Hence the interference pattern reappears and thus the scheme completes the quantum eraser experiment.

There is a practical utility of quantum eraser experiments in quantum computing and quantum cryptography. The qubit used in quantum computing/cryptography demands entanglement of two quantum states and the system must exist in these two states simultaneously and consequently these states must interfere. It is quite difficult to keep the system in a superposed state until needed. By utilizing the quantum eraser experiment this problem can be solved and interference can be maintained when desired.

Next, we discuss yet another experiment based on Feynman's idea (discussed above) or a Heisenberg light microscope providing 'which-way' information in Young's double-slit experiment with electrons or atoms. The basic element of this experiment[22] is a three-grating Mach–Zehnder atom interferometer (Figure 10) in which single photons are scattered from interfering de-Broglie waves, and the loss and revival of fringe contrast are measured as the separation of the interfering path at the point of photon scattering. In this experiment, the loss of coherence cannot be attributed to the momentum transferred in the scattering. It is due to the random phase shifts between two interfering paths. This is because the photons can be scattered into various modes of the reservoir so that coherence is not destroyed but gets entangled with final state of the reservoir. So selective observation of atoms which scatter photons in a restricted part of the accessible phase space, results in regaining fringe contrast.

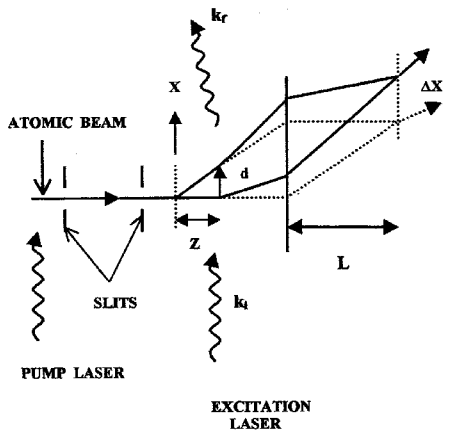

Figure 10. Schematic diagram of an atom (Mach–Zehnder) interferometer. Initial trajectories of atoms are shown as dotted lines; solid lines represent the atom trajectories after a photon (indicated by wavy lines with initial and final momentum k_i and k_f, respectively) is scattered from the atoms. Atom diffraction gratings are indicated by vertical dotted lines. Deflection Δx is used for measurement of final photon momentum projection k_x and Δk_x.

In this experiment[22], a Na atomic beam having almost a single velocity is produced in a seeded inert-gas supersonic jet. This beam is irradiated by a σ^+ polarized laser and the atoms are pumped into $F=2$, $m_F=2$ state. This beam travels through two slits (85 cm apart) for collimation (Figure 10). The atom interferometer consists of three nanofabricated diffraction gratings. By measuring the transmitted atomic flux through the gratings while varying their positions, intereference pattern gets recorded; contrast of these fringes along with the phase information is retrieved by data fit. Single-photon scattering (within the interferometer) by the atoms is obtained by exciting them to $F'=3$, $m_{F'}=3$ state using a σ^+ polarized laser beam. The atom then de-excites back to the ground state via spontaneous scattering. In order to study how the photon scattering affects atomic coherence as a function of separation d, the excitation laser beam is translated slowly along the atomic beam axis z and the contrast/phase of the fringes is determined at each point with and without spontaneous photon scattering. In the experiment, initially no correlation measurements were made between detected atoms and the scattered photon. As a result there was no change in the fringe contrast or the phase of the interference pattern. With increase in the separation of the interfering beams, the fringe contrast decreases sharply to zero. A further increase in d causes a periodic rephasing of interference and hence partial revival of contrast and a periodic phase modulation take place.

The next part of the experiment involves correlation measurement of atoms detected and the photons scattered into a restricted range of final direction. Normally, this is achieved by coincidence measurement of atoms with photons scattered in a specific direction. Due to technical reasons an equivalent experiment was performed in which, with the help of deflection of the atom, the final photon momentum projection as well as a small change in the momentum could be measured (see Figure 10). The outcome of such an experiment is partial regaining of the loss of coherence and hence the fringe contrast as d increases.

Two-photon JCM

Consider an atom which has a lower state $|g\rangle$ coupled to an excited state $|e\rangle$ by dipole-allowed transitions through intermediate states $|i\rangle$, $(i=1,2,...)$. The atom interacts with the em field in a cavity tuned to the frequency $\omega=(E_e-E_g)/2\hbar$, where $E_g(E_e)$ is the energy of the lower (excited) state. If the frequencies $(E_i-E_g)/\hbar$ and $(E_e-E_i)/\hbar$ (where E_i is the energy of an intermediate state $|i\rangle$) are sufficiently different from ω the atom acts like an effective two-level system absorbing and

emitting two photons of frequency ω each at a time. The effective Hamiltonian of the system is given by

$$H = 2\hbar\omega S_z + \hbar\omega a^\dagger a + \hbar g(a^{\dagger 2} S_- + S_+ a^2). \quad (25)$$

The parameter g is related to the two-photon matrix element and it is equal to the vacuum-Rabi frequency for two-photon transitions. With a suitable choice of the atomic transitions and cavity size, one can make it relatively large. In the two-photon maser: $g \sim 4000\ \mathrm{s}^{-1}$ for $44S \rightarrow 39P \rightarrow 39S$ transition in Rb.

The corresponding dressed states obtained by diagonalizing the Hamiltonian are given by[23] ($\hbar = 1$):

$$H|0, g\rangle = -\omega|0, g\rangle,$$

$$H|1, g\rangle = 0,$$

$$H|\psi_n^{\pm}\rangle = \lambda_n^{\pm}|\psi_n^{\pm}\rangle,$$

$$|\psi_n^{\pm}\rangle = \frac{1}{\sqrt{2}}[|n, e\rangle \pm |n+2, g\rangle],$$

$$\lambda_n^{\pm} = [\omega(n+1) \pm g\sqrt{(n+1)(n+2)}]. \quad (26)$$

The probability for an atom initially in the excited state $|e\rangle$ to remain in the excited state is

$$P_e(t) = \frac{1}{2}\left[1 + \sum_{n=0}^{\infty} P(n)\cos(2gt\sqrt{(n+1)(n+2)}\right]. \quad (27)$$

If the cavity field is in a coherent state $|\alpha\rangle$, then $P(n) = (\bar{n})^n e^{-\bar{n}}/n!$ and using $\sqrt{(n+1)(n+2)} \approx (n+3/2)$ we have

$$P_e(t) = \frac{1}{2}[1 - e^{-2\bar{n}\sin^2 gt}\cos(\bar{n}\sin(2gt) + 3gt)]. \quad (28)$$

There is complete revival of the Rabi oscillations after their collapse. Many other interesting effects such as self-induced transparency, adiabatic following in single as well as two-mode two-photon JCM have been predicted recently[23]. This model has been further investigated with driving field and a long time collapse and revival phenomenon have been observed in orbital motion[23].

Cavity quantum electrodynamics

In 1946, Purcell[24] pointed out that the spontaneous emission rate for an atom in a lossy cavity should be increased by the cavity Q-factor[24]. The fact that an atom is contained in a cavity can modify the rate of spontaneous emission, since the allowed modes into which the atom can radiate are different from those of infinite free space. A cavity of length d expels modes of wavelength $\lambda > 2d$. In the late sixties, some spectacular experiments using molecular monolayers deposited on reflecting plates showed that the rate of spontaneous emission near a mirror is a function of the distance from the mirror[25]. These results were also explained theoretically by both fully classical[12] and fully quantum mechanical treatments[26]. These and the other early papers[27] prompted the present cavity QED experiments and theory which are concerned with the effects of electomagnetic boundary conditions on atomic radiative properties. Enhancement of the spontaneous emission rate of a single atom prepared in a tuned cavity has been observed by Goy *et al.*[28]. Kleppner[29] had predicted suppression of spontaneous emission in an off-resonant cavity. Such suppression of spontaneous emission has also been observed experimentally by Hulet *et al.*[30] using an atomic beam of Rydberg cesium atoms passing between mirrors separated by about 0.2 mm. Before the beam entered the cavity, an $n = 22$ state of cesium was prepared by excitation with two dye lasers, and then the atoms were put into a 'circular state' with $|m| = n - 1$ using an adiabatic passage technique[30]. With such an anisotropic circular state preparation, the dipole moment for the $(n = 22,\ |m| = 21) \rightarrow (n = 21,\ |m| = 20)$ transition was parallel to the mirror planes, so that substantial suppression of spontaneous emission could be investigated. Here applicability of selection rule $\Delta|m| = -1$ definitely tells that the radiation is polarized perpendicular to the quantization axis defined by an electric field. The mirrors were separated by $230.1\ \mu\mathrm{m} = 1.02\ (\lambda/2)$, where λ is the zero-field transition wavelength. The transition wavelength was Stark-shifted with an electric field (small enough to avoid ionization) over a tuning range $\Delta\lambda/\lambda = 0.04$. The state of the atom emerging from the cavity was determined by field ionization, using the fact that the $n = 22$ and $n = 21$ levels have significantly different ionization rates. As λ was varied by application of an electric field from 0 to 3.1 kV/cm, a dramatic suppression of spontaneous emission was indicated for $\lambda/2L > 1$: the lifetime becomes about 20 times larger than in free space.

Experiments with transition wavelengths in the near-infrared have been performed using much smaller mirror spacings by Jhe *et al.*[31]. In these experiments, a cesium atomic beam prepared in the $5d$ level entered a cavity with mirror spacing $1.1\ \mu\mathrm{m}$, so that the $5d \rightarrow 6p$ transition wavelength of $3.4\ \mu\mathrm{m}$ was larger than the cavity cut-off wavelength $2L = 2.2\ \mu\mathrm{m}$. It was observed that the atoms passed through the cavity for 13 natural lifetimes without emission. Using an applied field λ could be varied, and it was confirmed that spontaneous emission was no longer suppressed when the dipole has a component perpendicular to the mirror planes.

Both inhibition and enhancement of spontaneous emission in the optical region have been observed using a spherical Fabry–Perot resonator. In this case, the rate of spontaneous emission into the solid angle subtended by the Fabry–Perot resonator was varied by tuning it through different resonances. Reported inhibition and enhancement factors were 42 and 19, respectively.

$E_0(\vec{r})$ as defined above is generally position-dependent, with its tangential component vanishing at the cavity walls. Its maximum value is inversely proportional to the square root of the cavity volume V. Large Ωs are obtained when small cavities of the size of the order of wavelength are used. In microwave cavities of centimetre size, typical values of E_0 are $\sim 10^{-3}$ V/cm and coupling these cavities to Rydberg atom with large electric dipoles yields Ω in the range 10^5–10^6 s^{-1}. With optical atomic transitions coupled to millimetre size Fabry–Perot resonators, Ω is in the range 10^6–10^7 s^{-1}.

As mentioned previously, coherent effects discussed hitherto occur when the atom field coupling exceeds the rate at which the atomic and field energies are dissipated by relaxation. The cavity damping is characterized by its rate ω/Q and one requires that $\Omega > \omega/Q$. With Q factors of the order of 10^{10}, coherent QED effects can be explored easily.

Pancharatnam phase in cavity QED

The quantum mechanical phases such as geometric phase (Berry phase)[32,33] and Pancharatnam phase[34] are topics of current interest. There are many examples of systems whose behaviour is specified up to a phase by certain parameters. The total phase acquired by the wavefunction of a quantum system in a cyclic or non-cyclic evolution contains two parts, viz. the dynamical phase part and the geometric phase part. The dynamical phase of the state vector of a system is Hamiltonian-dependent, but the geometric phase depends on the chosen path in space spanned by all the likely quantum states of the system. The Pancharatnam phase is important in the propagation of a light beam, where its polarization state is changing periodically[34,35].

The Pancharatnam phase for the entangled state for one- and two-photon JCM as described above shows interesting behaviour, and explicitly contains information about the statistics of the field and atomic coherence[36]. The Pancharatnam phase ϕ has both the dynamical (ϕ_d) and the geometric (ϕ_g) phase parts and can be defined between the vectors $\psi(0)$ and $\psi(t)$ as[34]

$$\phi_t = \arg\langle \psi(0) | \psi(t)\rangle. \tag{29}$$

The dynamical phase for an arbitrary quantum evolution from time $t=0$ to t is given by the time integral of the expectation value of the Hamiltonian over the time interval $t=0$ to t,

$$\phi_d = -\frac{1}{\hbar}\int_0^t \langle\psi(t)|\, H\, |\psi(t)\rangle \mathrm{d}t. \tag{30}$$

So, the geometric phase under Schrödinger evolution is given by

$$\phi_g = \phi - \phi_d. \tag{31}$$

Both the ϕ_d and ϕ_g are important in determining the behaviour of ϕ.

Assuming that both the levels of the two-level atom are equally populated initially, we have shown the behaviour of inversion and phase in Figure 11 for one-photon JCM. Figure 11 *a* depicts population inversion of a one-photon JCM in the coherent field, which exhibits the phenomenon of collapses and revivals of Rabi

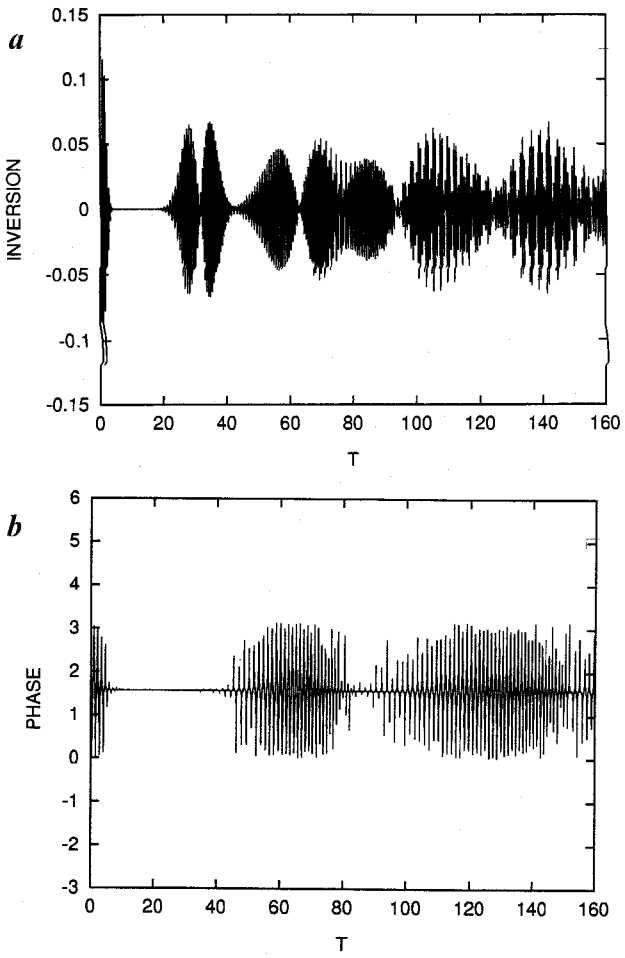

Figure 11. *a*, Population inversion for a two-level atom undergoing a one-photon transition as a function of scaled time T, with the cavity field initially in the coherent state having mean photon number 25 and the atom in symmetric superposition of its state; *b*, Pancharatnam phase as a function of scaled time T for the same system under similar conditions of parameters.

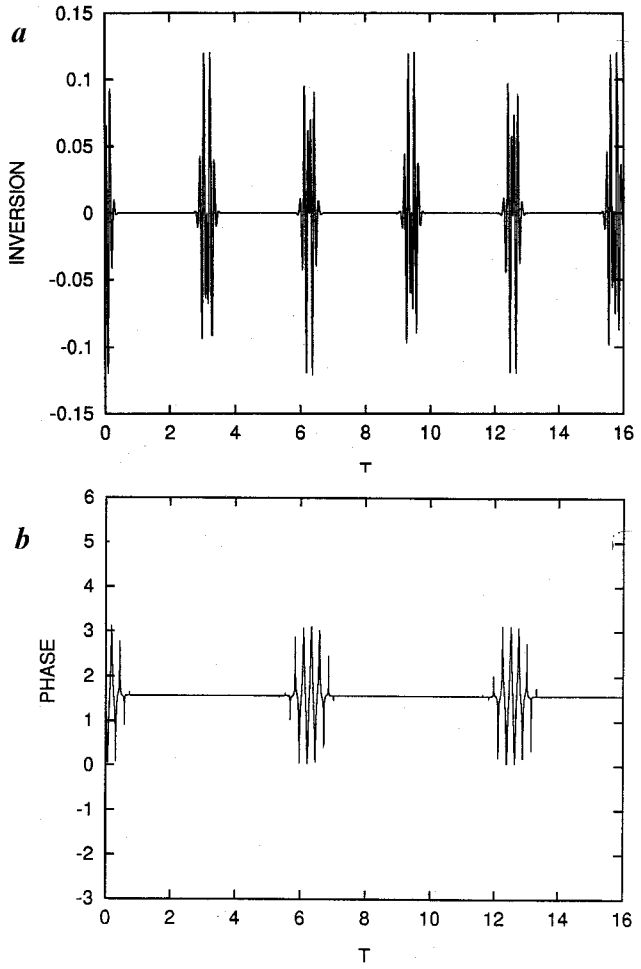

Figure 12. Same as Figure 11, but for an atom undergoing a two-photon transition.

oscillations. It is interesting to note that a similar behaviour is seen in the evolution of the Pancharatnam phase ϕ (Figure 11 *b*).

Figure 12 shows inversion for the two-level atom undergoing two-photon transition in the single-mode coherent field (the two-photon JCM) which exhibits the periodic collapse and revival phenomenon of Rabi oscillations with a period of π (Figure 12 *a*). However, it is important to note that the Pancharatnam phase (ϕ) evolution in T (Figure 12 *b*) for the two-photon JCM is also similar to the periodic collapse–revival phenomenon of Rabi oscillation, but with a period of 2π Thus the behaviour of the Pancharatnam phase (ϕ) is in contrast to the behaviour of the dynamical phase (ϕ_d) (eq. (30)). Also, if the atom is initially either in its lower or upper state only, then we do not observe any phase evolution for this system.

Thus, the Pancharatnam phase for a system of cavity-quantized field interacting with a two-level atom is quite sensitive to the initial conditions of its constituent sub-systems. If the initial conditions are such that they produce some kind of entanglement, only then does one observe Pancharatnam phase as well as the dynamical phase. In such cases, the phase ϕ can distinguish between different statistics of radiation in the cavity as well as the type of photon transition involved. Such entanglement is important in schemes to transmit quantum information, such as teleportation, quantum cryptography and quantum computation (qubits, etc.)[37]. The phases discussed above are physically observable interferometrically through a 'structured' approach[38] or can be estimated by other techniques of phase estimation[39].

New experiments in cavities and ion traps

Experiments conceived in cavities

The two basic and important properties of a high-Q cavity and a two-level atom coupled system are (i) the atom and the field evolve into an entangled state with high correlation between the two sub-systems, and (ii) these correlations may affect the internal as well as the external degrees of freedom of the atom interacting with the cavity.

Possible realization of these ideas are now devices like an 'inverse optical Stern–Gerlach' apparatus (where the usual magnet is replaced by a cavity) or a 'Young's double-slit interferometer' for matter waves with retarding plates made of a cavity containing a quantum field adiabatically coupled to a beam of atoms. These devices make it possible (i) to measure photon number in the cavity, (ii) to prepare Fock state of the field, and (iii) to generate a variety of non-classical states, e.g. the 'Schrödinger cat states' of radiation. These are merely not 'Gedenken' experiments, but have become practically feasible with the state-of-the-art technology related to atomic beams and high finesse cavities in the microwave as well as in the optical domain. Such experiments have been conceived and are being carried out at Ecole-Normale Superieure in Paris[40].

The basic system involved is a two-level atom of transition frequency ω_0 resonant or near resonant with a single mode of high-Q cavity of frequency ω The essential parameter is the 'Vacuum field Rabi frequency' $\Omega(\vec{r})$ which represents the rate at which the atom and the initially empty cavity reversely exchange a photon (as discussed earlier). This coupling $\Omega(\vec{r}) = pE_0(\vec{r})/\hbar$, where p is the dipole matrix element between levels $|e\rangle$ and $|g\rangle$ and $E_0(\vec{r})$ the vacuum field rms amplitude in the cavity which depends on the geometry.

Let us invoke the dressed states defined earlier. Apart from the ground state $|g, 0\rangle$, all other system eigenstates appear to be 'entangled', with the internal state of the atom correlated to the state of the photon field. The eigenstate $|\psi_n^{\pm}\rangle$ (and energy $\lambda_n^{\pm}$) evolves continuously

as the atom moves across the cavity. If the atom and cavity are detuned by a small mismatch δ then $|e, n\rangle$ and $|g, n+1\rangle$ states are non-degenerate outside the cavity. As the atom moves inside, these states repel each other and evolve into the $|\psi_n^{\pm}\rangle$ coupled states. This is shown in Figure 13, where a microwave cavity is assumed to sustain a $\sin(\pi z/L)$ mode which vanishes on the cavity axis at $z = 0$ and $z = L$, and has a maximum at the cavity centre. We are assuming a small negative detuning δ The energy levels are shown in two-state manifolds whose maximum separation at the cavity centre is $2\Omega_0\sqrt{n+1}$ (Ω_0 is the vacuum Rabi frequency at this point). If the atom–cavity system is initially prepared in $|e, n\rangle$ or $|g, n+1\rangle$ state and the atomic motion is slow enough, it will follow one of the atom–cavity levels. In this adiabatic approximation the total internal energy is either decreased or increased as the atom moves inside the cavity[40].

Note that the eigen energies ($\lambda_n^{\pm}(\vec{r})$) play the role of potential energies for the motion of the atom in the cavity field. The atom is either attracted in the cavity ($|\psi_n^-\rangle$ state) or expelled from the cavity ($|\psi_n^+\rangle$ state). This force experienced by the atom being proportional to $\sqrt{n+1}$ is, in fact, quantized taking discrete values depending on the photon number.

A wave packet $\psi_{e,n}(r, t)$ associated with the external motion of atom obeys the Schrödinger equation

$$i\hbar\frac{\partial}{\partial t}\psi_{e,n}(r,t) = \frac{-\hbar^2}{2m}\Delta\psi_{e,n}(r,t) + \lambda_n^+(r)\psi_{e,n}(r,t). \quad (32)$$

This wave packet follows the trajectory of a classical particle in the same potential $\lambda_n^+(\vec{r})$. The atom packet will cross the cavity if the initial atomic kinetic energy exceeds the potential barrier height.

After exiting from the cavity the position of the centre of the wave packet depends on the potential seen during cavity crossing and hence the photon number n. So, we have an elastic atom–cavity 'collision' whose 'final' external state contains information about the 'inverse Stern–Gerlach' experiment, because the field gradient itself is the quantum object having discrete internal state (photon number) and the atomic trajectories get correlated to these numbers. A conceptual experiment is shown in Figure 14. Atoms enter the cavity on one side and get deflected along different trajectories depending on the photon number in the cavity[40].

An interesting case is when the cavity is initially in the coherent superposition of photon states $|\phi\rangle = \sum_n C_n|n\rangle$. In this case

$$\psi_e(\vec{r}, t) = \sum_n C_n\psi_{e,n}(\vec{r}, t), \quad (33)$$

provided the trajectories corresponding to different n values are well separated. The detection of the atom at a given point will produce a 'collapse' of this wavefunction and reduce the field in the cavity to a well-defined n value.

Another approach to determine n is shown in Figure 15, which is based on atomic wave packet dephasing with cavity QED experiment. The figure shows a wave packet (X) impinging on a cavity containing n photons. After exiting from the cavity, the packet is dephased (shown as Y) by an amount $\Delta\phi(n)$ given by

$$\Delta\phi(n) = \frac{m}{\hbar k}\int \Omega_0(\vec{r})\sqrt{n+1}\, dz, \quad (34)$$

for small δ Here, k is the momentum of the atom ($k = 2\pi/\lambda_{DB}$, where λ_{DB} is atomic de-Broglie wavelength). A dephasing of 2π is equivalent to a delay of the atom wave packet equal to λ_{DB} ΔZ (packet width). Measuring $\Delta\phi$ is a sensitive way of determining photon number in the cavity[40].

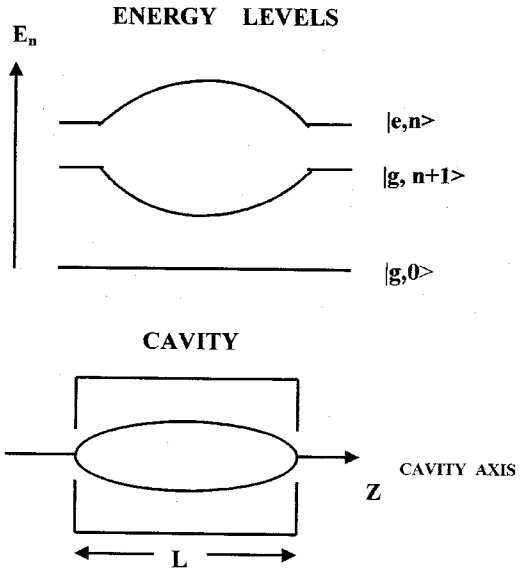

Figure 13. A cavity having sinusoidal mode sustained in the cavity (bottom). (Top) Energy levels of the atom–cavity system as a function of length along the cavity axis.

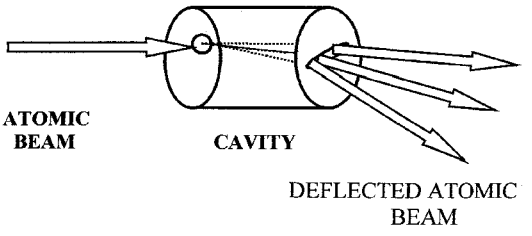

Figure 14. Schematic diagram of inverse Stern–Gerlach experiment. Note that the atoms enter the cavity at one end near a side and get deflected along different trajectories which are dependent on the photon number.

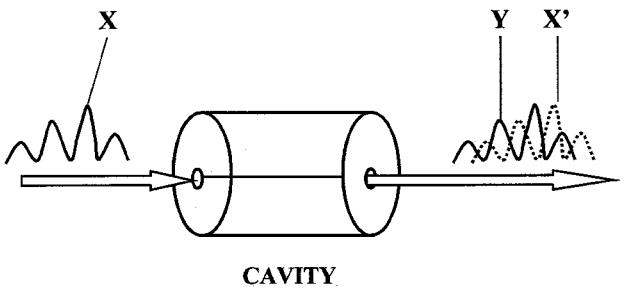

Figure 15. Dephasing of matter wave packet (X) adiabatically crossing a cavity. The phase difference is evident in the wave packet marked Y. X′ represents the wave packet as it would be at the same time as in Y, provided there is no cavity in the path.

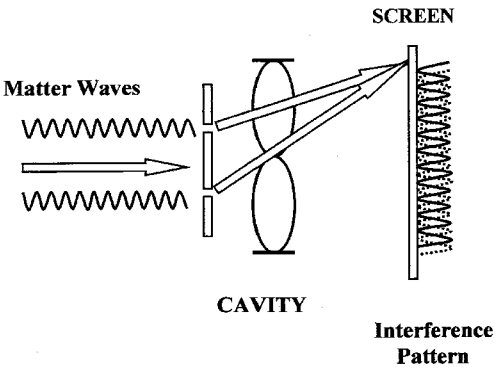

Figure 16. Apparatus for matter wave interferometry. Upper slit is designated as slit 1 and the lower as slit 2 in this case. Phase shift can be clearly seen on the screen.

To measure the phase shifts, interferometry is the best choice. A simple scheme is shown in Figure 16, where an atom wave packet is sent through a pair of Young's double-slit apparatus. The cavity, whose field is to be measured, is placed after the slits. The cavity mode is so chosen that there is a field antinode behind slit 1 and a field node behind slit 2. The atom wave is dephased only if it follows the path through slit 1. The atoms are sent through this set-up one by one, and their position on the detection screen is recorded. The recorded pattern of atoms results in the interference pattern. When this interference pattern is compared with the interference pattern of atoms recorded without the cavity field, there will be a spatial phase shift observed, which will directly yield the dephasing produced by the cavity field[40].

If the cavity is in a coherent superposition of Fock states, then something interesting happens. In this case, there is an initial (photon) n-indeterminacy and the phase of fringe pattern is not defined *a priori*. The first atom can be detected at any point in the detector plane. The photon 'reveals' itself as successive atoms cross the apparatus and get recorded, making the fringe pattern to progressively emerge on the screen. This is a typical example of a quantum nondemolition (QND) measurement of the field intensity.

There are other variations of this experiment. For instance, one can use the Ramsey fringe interferometer instead of Young's apparatus[40]. To realize this method, a superposition state comprising states $|e\rangle$ and $|g\rangle$ must be prepared, then its evolution in the cavity should be allowed. The resulting phase shift of atomic dipole processing at the Bohr frequency between $|e\rangle$ and $|g\rangle$ is measured. This shift proportional to the number of photons will provide QND information on the cavity field. The detuning of atomic frequency and cavity-mode frequency is large compared to the atom–field coupling so that there is no loss of photon. At the same time atom–field coupling, is quite sufficient to induce substantial shift in levels $|e\rangle$ and $|g\rangle$ (which eventually leads to dressed energy eigenstates), once the atom enters into the cavity. In this particular 'Ramsey method', separated oscillatory fields are utilized for the purpose of preparation of superposition state of $|e\rangle$ and $|g\rangle$, and detection of phases of the amplitudes associated with $|e\rangle$ and $|g\rangle$ state (Figure 17 *a*). The cavity is sandwiched between two zones, RAM1 and RAM2, where auxiliary fields are applied to the atoms.

Atoms initially in level $|e\rangle$ are sent across the cavity along a single, well-defined trajectory. The cavity is interposed between two 'Ramsey zones', RAM1 and RAM2 in which a classical field (laser) or the auxiliary field is applied. In RAM1, a $\pi/2$ pulse interacts with the atoms and prepares them in a linear superposition of their states $|e\rangle$ and $|g\rangle$ before they enter the cavity CAV. After entering the cavity, each of these states is dephased by a different amount by the cavity field. As a result, the atom packet 'splits' into two overlapping components dephased by different angles. After the atom leaves the cavity, the second Ramsey zone RAM2, coherently mixes the two components again, in such a way as to restore the initial state $|e\rangle$, when the cavity dephasing is precisely zero (or a multiple of 2π). This is done by a second $\pi/2$ pulse in RAM2. After the second zone, the atoms are detected selectively by two counters sensitive to levels $|e\rangle$ and $|g\rangle$, respectively. The probability of finding the atom in either level is a sinusoidal function of the cavity dephasing. The experiment thus records fringes versus time spent by the atoms in the cavity and leads to an elegant QND measurement of the photon number, i.e. counting the photons without destroying them. The same set may be used to detect 'photon quantum jumps'[40].

The 'resonant' method using Ramsey interferometry has been applied to measure a single photon without destroying it[41]. This scheme is slightly different from what we have discussed above and is only feasible for single photons. Hence it is called a restricted QND

scheme. Here, a three-level atomic configuration is exploited to carry out QND measurement. In an experiment recently carried out by Haroche's group, an open geometry cavity having two electrically isolated spherical niobium mirrors has been used to demonstrate this experiment. The system is cooled to 0.6 K in a He cryostat to control the average thermal photons to be less than 0.02 or so in the cavity. The atomic source is an effusive Rb atomic beam pumped by a laser for velocity-selected excitation to circular Rydberg state having principal quantum number $n = 50$ (for state $|g\rangle$) or $n = 51$ (for state $|e\rangle$). The transition frequency of interest and the labelling of atomic levels are depicted in Figure 17 *b*.

The cavity is in resonance with $|g\rangle \rightarrow |e\rangle$ transition, but non-resonant with $|g\rangle \rightarrow |i\rangle$ transition, and it contains either 0 or 1 photon. The atom initially in state $|g\rangle$ enters the cavity and the velocity of the atom is so adjusted that the interaction time satisfies the condition $\Omega t_{\text{int}} = 2\pi$ (Ω is the Rabi frequency between levels $|e\rangle$ and $|g\rangle$). The Ramsey fringes on the transition $|g\rangle \rightarrow |i\rangle$ are recorded by the method discussed above. The Ramsey zone fields are applied to $|g\rangle \rightarrow |i\rangle$ transition in this case, rather than the $|g\rangle \rightarrow |e\rangle$ transition. The fringe patterns recorded when there is 0 and 1 photon in the cavity has a phase shift difference of π So, the maxima of 0 photon case interference pattern become minima of 1 photon case and vice versa. This effect of measuring phase shift in interference pattern gives rise to QND measurement of single photon and it is called single-photon QND (SP-QND) scheme[41]. The unrestricted scheme of QND measurement for an arbitrary photon number with this method is yet to be realized experimentally. Such an unrestricted scheme will not be based on the 'resonant method', but the atom–cavity field detuning will be maintained so that the photon absorption can be completely suppressed.

Conditional phase gate and QND: The photon–atom system in these experiments behaves as quantum bits (qubits) carrying binary information. The Rabi pulse having pulse area 2π acts as a quantum phase gate (QPG)[42] and causes the following transformations on the four combined atom–photon states: $|0, g\rangle \rightarrow |0, g\rangle$, $|1, g\rangle \rightarrow e^{i\pi}|1, g\rangle$, $|0, i\rangle \rightarrow |0, i\rangle$, $|1, i\rangle \rightarrow |1, i\rangle$. This type of a gate together with unitary rotations, when applied on each qubit, can produce any unitary two-qubit operation. Also, the SP-QND measurement scheme obeys the conditional dynamics of controlled-not (C-NOT) gate. The C-NOT gate is an important constituent of a quantum computer.

QND and preparation of Fock state field: The method of QND measurement is also useful to prepare Fock state of the em field. For this purpose, a cavity with almost infinite quality factor (Q) sustaining a definite photon number distribution $p_0(N)$ is employed and the atomic beam is allowed to pass through it. This atomic beam is almost monokinetic and having a fixed velocity. The states of the atoms are monitored when they leave the cavity. Any measurement carried out on atoms changes the cavity field density operator and hence the photon number distribution. Thus after the nth atom leaves the cavity and its state is measured, the photon number distribution reduces to $p_n(N)$. Detection of each atom produces partial reduction of field density operator as the atom–field combined density operator is entangled. As more and more atoms pass through, many photon number states get lost from the original photon number distribution and only one particular photon number state is left behind, and the field is reduced to a Fock state[40]. This has also been simulated by a numerical experiment employing Monte Carlo simulation method. In another numerical simulation experiment by one of us, in which all the atoms are projected into their excited state at the time of detection, we get Fock state generation in the cavity (Figure 18).

Schrödinger cats: In the Ramsey set-up, the atom crosses the cavity in a linear superposition of its states $|e\rangle$ and $|g\rangle$. After the atom leaves the cavity and before it reaches the second Ramsey zone, the atom–field system is in the 'entangled' state:

$$\psi_I = \frac{1}{\sqrt{2}}[|\, e, \alpha e^{i\phi}\rangle + |\, g, \alpha e^{-i\phi}\rangle]. \tag{35}$$

The evolution of the system in this second zone has the effect of 'splitting' the levels $|e\rangle$ and $|g\rangle$ again, so that the new state becomes

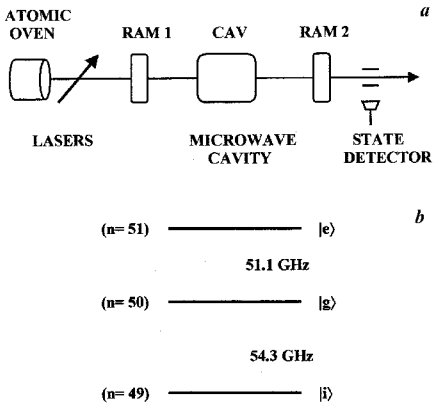

Figure 17. *a*, Schematic diagram for measuring photon number in the cavity with quantum nondemolition (QND) method. Atomic beam is pumped by the lasers to prepare them in Rydberg state. RAM1 and RAM2 are two Ramsey field zones and CAV is the microwave cavity followed by a state detector using field ionization technique for detection; *b*, Schematic of atomic levels and the microwave transitions involved in resonant (or restricted) QND method.

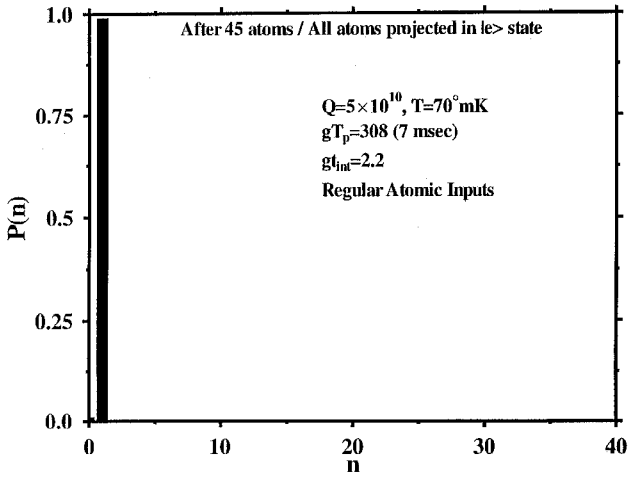

Figure 18. Simulation of Fock state generation for the conditional measurement of all atoms in the excited state. The field is initially in the thermal state having photon number distribution used in eq. (10) at $T = 70$ mK and the process is independent of interaction time.

$$\psi_{II} = \frac{1}{\sqrt{2}}[|\, e, \alpha e^{i\phi}\rangle + |\, g, \alpha e^{i\phi}\rangle] + [|\, g, \alpha e^{-i\phi}\rangle - |\, e, \alpha e^{-i\phi}\rangle]). \tag{36}$$

Detection of the atom in level $|e\rangle$ ($|g\rangle$) then leaves the field in one of the final (not normalized) states:

$$\psi = |\alpha e^{i\phi}\rangle \mp |\alpha e^{-i\phi}\rangle. \tag{37}$$

When $\phi = \pi/2$, the two components have opposite instantaneous amplitudes. These states are known as 'Schrödinger cat' states and are non-classical. There are schemes in which one can produce general states like

$$\psi_{\pm}^{s} = |\alpha + \beta\rangle \mp |\alpha - \beta\rangle. \tag{38}$$

In particular, when $\beta = \alpha$ we have the state $|2\alpha\rangle + |0\rangle$, which is the sum of the coherent state and the vacuum field. Note however, that such states must be prepared and analysed in a time interval short compared to their quantum coherence decay times. This condition can be satisfied for microwave superconducting cavities. Interest in such states is because it is an experiment investigating test ground of quantum mechanics at the frontier between macroscopic and microscopic physics[40].

In experiments by the NIST group[43] Schrödinger cat-like state of matter has been generated at a single-atom level. In this experiment, a $^9Be^+$ ion was trapped and cooled down to its 'zero-point' energy by employing laser cooling and then a superposition of spatially separated coherent harmonic oscillator states was produced with the help of a sequence of pulses. Each spatially-separated state or the wave packet is correlated with a particular internal state of the atom. The production of Schrödinger cat state is analysed with the help of additional laser pulse that couples internal states and gives rise to quantum interference of wave packets. In this method of production of Schrödinger cat state, no conditional measurement has been imposed.

To achieve the above methodology of production of Schrödinger cat state, a coaxial-resonator RF ion trap has been used to confine a single $^9Be^+$ ion with harmonic oscillator frequencies $(\nu_x, \nu_y, \nu_z) \sim (11.2, 18.2, 29.8$ MHz) along the principal axes of the trap. The ion is then laser-cooled so that it reaches the ground state of the motion. The atomic states of interest (Figure 19 *a*) are $^2S_{1/2}$ $(F = 2, m_F = -2)$ and $^2S_{1/2}$ $(F = 1, m_F = -1)$ defined as $|D\rangle_i$ and $|U\rangle_i$, with separation $\omega_I = 1.25$ GHz. These states are Raman-coupled through an excited level $^2P_{1/2}$ $(F = 2, m_F = -2)$, which acts as a virtual level. The Raman coupling is provided by means of off-resonant laser beams A and B. By tuning the Raman beam difference frequency near ω_I and adjusting the exposure time of lasers A and B, the internal states can flip or split/recombine. A pulse with area $\pi/2$ on the carrier actually splits the wave function into an equal superposition of states $|D\rangle_i|0\rangle_e$ and $|U\rangle_i|0\rangle_e$ (where $|0\rangle_e$ represents initial zero-point state of motion). Since these beams are co-propagating, they do not significantly affect the motion of the ion. When the Raman beam difference frequency is tuned near ω_g and displacement beams B and C are applied, then the initial zero-point state of motion is displaced to a coherent state. The polarization of Raman beams A, B, C is so adjusted that the displacement beams (B and C) affect only the motional state correlated with $|U\rangle_i$ internal state and provide quantum entanglement of the internal state with external motional state.

We can say that the displacement beams excite the $|0\rangle_e$ state associated with the state $|U\rangle_i$ to a coherent state $|\beta e^{-i\theta/2}\rangle_e$. After this, a pulse with area π on the carrier is applied and it swaps the internal state in the superposition. In the next step, another displacement beam is applied which shifts the state of motion correlated with $|U\rangle_i$ to a second coherent state $|\beta e^{i\theta/2}\rangle_e$ and finally a $\pi/2$ pulse on the carrier combines these coherent states (see Figure 19 *b* for these steps). After each preparation cycle, the internal state of the atom independent of its motional state is determined by the detection beam D. Once a Schrödinger cat state is formed (step 5 in Figure 19 *b*), then it contains quantum interference in it. Hence the formation of the Schrödinger cat state can be diagnosed by measuring quantum state interference using detection of ion in $|D\rangle_i$ internal state for a given value of θ. The experiment is repeated several times while slowly changing the phase θ and the interference pattern (by measuring the signal) is recorded. That tells us whether 'even' or 'odd' Schrödinger cat state has been produced.

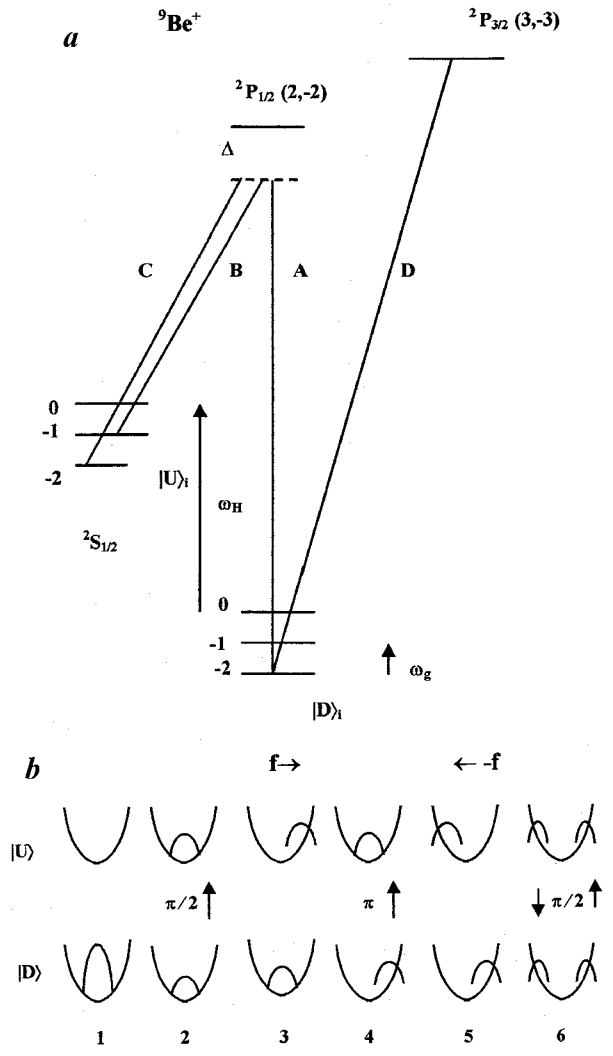

Figure 19. *a*, Energy levels of a trapped $^9Be^+$ ion. A two-photon Raman coupling between the levels $^2S_{1/2}$ (F, $m_F = 2$, -2) and $^2S_{1/2}$ (F, $m_F = 1$, -1) is denoted by $|D\rangle_i$ and $|U\rangle_i$, respectively (the hyperfine ground states) is shown. The difference frequency of laser beams A and B is $\omega_H = 2\pi \times 1.25$ GHz and the difference frequency of the displacement Raman beam B and C is $\omega_g = 2\pi \times 11.2$ MHz. Laser beam D is the detection beam to know the internal state of atom after each cycle. *b*, Atomic wave packet entangled with internal states $|D\rangle_i$ and $|U\rangle_i$ during Schrödinger cat state formation. Wave packets are shown at various positions of harmonic trap parabolas; 1, Initial wave packet for the laser-cooled ion in its ground state of motion; 2, A $\pi/2$ pulse causes splitting of the wave packet; 3, $|U\rangle_i$ wave packet is displaced to a coherent state by a displacement beam (with a force of displacement f); 4, $|D\rangle_i$ and $|U\rangle_i$ wave packets are swapped following a π pulse; 5, $|U\rangle_i$ wave packet is displaced to a coherent state by another displacement beam (with a force of displacement $-f$). This displacement is out of phase with that in 3. The state corresponding here in 5 is a Schrödinger cat state; 6, $|U\rangle_i$ and $|D\rangle_i$ are eventually combined following a $\pi/2$ pulse. This is done to verify the Schrödinger cat state formation in step 5.

Besides this, the NIST group has also demonstrated creation of thermal, Fock, coherent and squeezed states of motion of the harmonically-bound $^9Be^+$ ion. The last three states are coherently prepared from an ion which has been initially laser-cooled to zero-point of motion. We refer readers to ref. (43) for more details.

Analogies to cavity QED

Quantum mechanical wave packets are analogous to a spatially localized classical particle travelling along a well-defined trajectory. The uncertainty principle places a limitation on this localization. For bound systems excited well above their ground states, this may not be a stringent limitation. The problem is that generally a wave packet does not remain localized, but spreads. In some cases, however, the spreading reverses itself and the wave packet relocalizes again. An example of this is the decay and revival of classical coherence predicted and observed in the micromaser realization of the JCM. The decay and revival here correspond to the Rabi oscillations of the inversion of a Rydberg atomic transition. An analogous case is the observation of the decay and revival of a spatially localized Rydberg electronic wave packet[44]. This revival may be attributed to the discreteness of the quantized energy states. In JCM it is the quantized nature of the cavity field, while in the present case it is the quantized nature of atomic energy levels. Another necessary feature in both cases is the fact that the coherence superposition state is made up of frequency components that are almost equally spaced. In the experiment, the Rydberg electronic wave packet is formed in the excited states of atomic sodium. The wave packet is excited by a one-photon process from the ground state to the Rydberg series by a short, ultraviolet pulse ($\tau_{pump} = 15$ ps, $\lambda = 2858$ Å). The evolution of the wave packet is the photoionization signal as a function of delay time. The Rydberg states have a range of values for the principal quantum number n, with average value of $\bar{n}$ ($\bar{n} = 65$ in this case). The resulting wave packet has the appearance of a shell oscillating between the nucleus and the outer turning point with the classical orbital period $\tau_0 = 2\pi\bar{n}^3$ au. The period of the decay and revival is $\tau_{dr} = \frac{2}{3}\pi\bar{n}^{-1}$ au.

Another example is the behaviour of a single trapped ion constrained to move in a harmonic oscillator potential and undergoing laser cooling at the node of the standing wave. Under conditions in which vibrational amplitude of the ion is much less than the wavelength of light (Lamb–Dicke limit), this problem is mathematically equivalent to the JCM, with negligible damping of the oscillator.

This system can be used for investigating several features of JCM which have so far been studied only in the context of cavity QED. For example, it should be possible, in principle, to prepare a Fock state corresponding to the quantized motion of the ion in analogy to preparation of the photon number state in the cavity QED[45] (see later in the article). Likewise, one can think of a

scheme for preparing coherent squeezed state of motion of the trapped ion based on the multichromatic excitation of ions by standing and travelling wave light fields (see ref. 43). The squeezed state is produced when the beat frequency between two standing-wave light fields is equal to twice the trap frequency, and is indicated by a 'dark resonance' in the fluorescence emitted by the ion. Also, the nonlinear coherent states (NCS) of the harmonic oscillator, which could be realized in the motion of trapped atoms have been introduced[46]. The NCS can display nonclassical properties such as amplitude squeezing and quantum interferences. Various properties of NCS, including entropies, phase properties and the presence of 'number cat' within number-phase Wigner formalism have been reported recently[46].

Cold atoms in cavity QED: Quantum measurements and quantum traps

Recently, experiments in cavity QED have been pursued using cold atoms from a Cs magneto-optical trap (MOT) falling one by one through a small high-finesse optical cavity (Figure 20), with just one photon (on the average) present in the cavity[47]. The cavity atoms are excited by a weak on-resonant field which is detected as transmission signal using quantum-limited heterodyne techniques. The transit time of the atoms in the cavity waist of 45 μm is about 100 μs. The radius of curvature of the mirrors of cavity was 100 cm, with finesse of the order of 200,000. It is the strong atom–field coupling $g_0 = 2\pi(11)$ MHz together with long transit time that has provided a means to observe single atoms in real time in the transmission of weak probe field. The atom–field coupling is varied spatially in the cavity and the combination of spatial and temporal resolution becomes promising to explore quantum limits to the position measurements of single atoms. Further experiments related to continuous quantum measurements can be visualized with such systems.

Trapping and laser cooling of atoms is one of the research areas of current interest in quantum optics. As far as optical cavity QED is concerned, in the strong coupling regime ($\hbar g_0 \quad k_B T_{\text{Doppler}}$), a single quantum of photons is good enough for the laser-cooled atoms to profoundly affect the atomic centre-of-mass motion which can change the cavity field significantly. Thus it is possible to trap the atoms in the cavity with single-photon field, as the spatial variation of the coupling energy provides mechanical potential of depth $\sim\hbar g_0$. In optical cavities $\hbar g_0 \sim 50$ $k_B T_{\text{doppler}} \sim 6$ mK, and this is quite large compared to the energy of the laser-cooled atoms. Thus, it opens a way to realize a quantum trap for the individual atoms in the cavity (details of the experiment are given later in the article). The utilization of cold-trapped atoms in cavity QED experiments will be useful in determining quantum-limited measurements of atomic positions and in quantum state synthesis. Also, such experiments would be useful in realizing diverse protocols in quantum information sciences.

Trapping of an atom with single photons: In recent experiments (Figure 21 *a*) by Pinkse *et al.*[48] (Rempe's group at MPQ, Garching) and Hood *et al.*[47] (Kimble's group at CalTech), using a high-finesse optical cavity sustaining a Gaussian TEM_{00} mode, the trapping of an atom has been demonstrated with light field containing

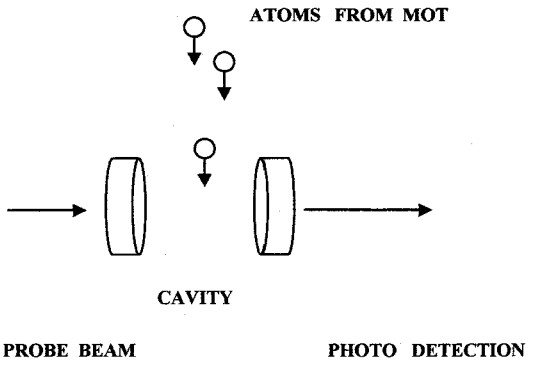

Figure 20. Schematic of the experiment in which atoms from the magnetic-optic trap (MOT) are dropped in the cavity. The cavity is probed with a weak field which is resonant with cavity frequency and atomic transition frequency.

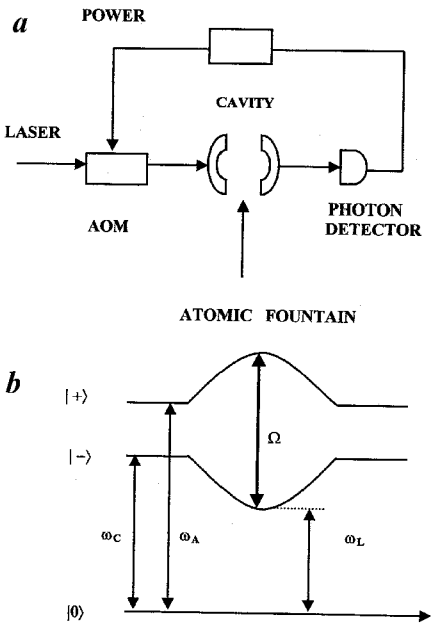

Figure 21. *a*, Experimental set-up showing trapping of an atom with single photon. Atoms are put into the high finesse cavity with a fountain. The acousto-optic modulator (AOM) is triggered due to the presence of the atom in the cavity and thus the laser light intensity is increased. *b*, The ground state is $|0\rangle$ and the first set of dressed states is $|\pm\rangle$. Atomic transition frequency, cavity frequency, laser frequency and Rabi frequency are indicated as ω_A, ω_C, ω_L and Ω, respectively.

on the average just a single photon. The trapped atom having oscillatory motion in the light field thus induces oscillations in the transmitted light intensity. The oscillations are caused due to the atomic motion within the cavity mode. Such kind of trapping is possible, i.e. a single atom trapped by an intracavity field having mean photon number of the order of 1, as the coherent coupling energy $\hbar g_0 = 5.3$ mK (g_0 is atom–field coupling coefficient) is larger than the atomic kinetic energy for the cold atom that is going into the cavity[48]. There are certain crucial differences between the usual laser cooling and trapping and its counterpart in the cavity QED domain of strong atom–field coupling. In free space it is just the nonlinear response of the atom, while in the cavity QED system it is the combined response of the atom and the cavity providing single quantum force just appropriate to trap the atom. Another difference is that in the cavity QED experiment it is possible to sense atomic motion in real time with very high signal-to-noise ratio, because of strong coupling.

The interaction of a single two-level atom with a single-mode field is well described by the Jaynes–Cummings model discussed earlier. The dressed states $|\pm\rangle$ and energies arising in this model are shown in Figure 21 *b*. The spatial variation of the dressed energies is governed by the spatial profile of the cavity field mode, which is a Gaussian. So, the cavity mode function has a maximum at the antinode (at the centre of the cavity) where the atom–field coupling coefficient has value g_0. The spatial variation in the dressed energy profile of state $|-\rangle$ represents a pseudo potential well of depth larger than the kinetic energy of atoms. So, when the atom is near the cavity centre, then driving it at frequency ω_L, populates the state $|-\rangle$ and atoms with kinetic energy $< \hbar g_0$ will be trapped. The atom and cavity thus form a bound quantum state in the potential well, and a 'molecule' of a single atom and the cavity is prepared, in which the atom and the cavity are sharing on the average one photon excitation and the centre of mass motion is bounded.

In the experiment of Pinkse *et al.*[48], the experimental set-up consists of (Figure 21 *a*) a high-finesse ($\sim 4.3 \times 10^5$) optical cavity in which a fountain of laser-cooled ^{85}Rb atoms (which is pulsed) is injecting very slow atoms (~ 20 cm s^{-1}) into the cavity. The cavity length is about 116 μm, so the transit time of the atom is about 0.12 ms. The cavity is undergoing active stabilization and the atoms are optically pumped into the state $5^2S_{1/2}$ ($F = 3$, $m_F = 3$). The cavity is sustaining a circularly polarized Gaussian-shaped TEM$_{00}$-mode laser beam which is near-resonant with the transition $5^2S_{1/2}$ ($F = 3$) $\leftrightarrow$ $5^2P_{3/2}$ ($F = 4$) at $\lambda = 780$ nm. An acousto-optic modulator is employed to control the intensity and the frequency of this light. The strength of atom–field coupling is $g_0 = 2\pi \times 16$ MHz, atomic damping rate $\gamma_0 = 2\pi \times 3$ MHz and the cavity damping coefficient $\kappa = 2\pi \times 1.4$ MHz. The potential depth for trapping an atom in this case is limited to $\hbar g_0$. In this experiment, as soon as an atom enters the cavity and is detected, the cavity triggers an external feedback switch and the laser intensity is increased. By doing so, the kinetic energy of the atom is compensated by the increased potential barrier. In order to demonstrate trapping, one requires the presence of the restoring force which is evident in the oscillatory motion of the atom or eventually in the laser transmission signal. With larger laser intensity (about 300 pW), the atom remains for about 1.7 ms in the cavity. Laser transmission power with respect to time is recorded in the experiment and information about the time-dependent atom–field coupling and the atomic trajectory is obtained. To better understand this experiment, quantum-jump Monte Carlo (QJMC) simulation was carried out. Based on the analysis of atomic motion it has been concluded that with oscillatory transmission signals, single atoms are actually trapped with light field having one or two photons. The limitation of the trapping time is governed by the spontaneous emission kicks by which the atom escapes radially. Some feedback-based cooling techniques can prevent such phenomena. Potentially, such a system of single particles trapped in a high finesse cavity has applications in quantum communications, to engineer arbitrary state of the em field and to generate a bit of stream of single-mode photons.

The experiment by Hood *et al.*[47] is quite similar to what we have discussed above. Instead of Rb atom fountain, they used Cs atoms captured in a magneto-optical trap (MOT) and then dropped them to a high finesse optical cavity. In this experiment, besides all other observations as discussed above, they proposed time-resolved microscopy or the atom–cavity microscope (ACM). By measuring the cavity transmission power of the laser in the presence of a single moving atom within the resonator, the real time recording of photocurrent is obtained[47]. Then an inversion algorithm is applied to this recorded data from which the position of the single atom is deduced. This implies that the cavity field acts as a microscope in tracking down the atomic motion in real time. In their experiment Hood *et al.*[47] obtained spatial resolution of 2 μm attained in 10 μs. The ACM has a potential application to track molecular dynamics in real time for a single molecule within the cavity and could provide information about molecular conformation also.

Role of cavity QED experiments in particle–wave duality of non-classical light

In a recent experiment[49] conditional homodyne detection has been carried out which combines detection of light as a particle (photocounts) along with the detection

of light as a wave (homodyne detection of wave amplitude). Thus this experiment (Figure 22) simultaneously addresses both the particle and wave attributes of a fluctuating light beam. Measurements of $g^{(2)}$ (the second-order intensity–intensity correlation) and squeezing separately can be seen as addressing the particle and wave attributes separately, while their simultaneous measurement addresses both the attributes together and hence runs into the expected difficulties of interpretation due to mutual inconsistency of the two attributes. Cavity QED is important since it provides the means to construct a source of light with the sort of quantum fluctuations needed to see this wave–particle conflict in the laboratory. When this experiment is compared with the standard textbook illustrations of wave–particle duality, perhaps the most important difference to note is that this experiment relies on the two-particle correlations of quantum fields, while usually wave–particle duality is presented in single-particle terms (the photon goes either through one slit or another). The perspective relies on experimental techniques that did not exist during the early years of quantum mechanics. For the correlations observed with the equipment shown in Figure 22, one needs to have a composite notion like the two-particle wave in order to take care of both the discrete triggering event and the continuously measured amplitude[49].

Cavity QED experiments for preparing Fock states of radiation

Fock states or the number states of the radiation field are characterized by a fixed photon number. Usually all other quantum states of the radiation field, e.g. coherent, thermal, binomial, etc. are a linear superpositions of various Fock states with different weightage factors. Thus the Fock state is the most fundamental quantum state. In ion traps, the Fock states associated with vibrational motion of the ions could be observed readily[43], but in order to see the Fock state of radiation field in the cavity QED experiments, care has to be taken to reduce the losses in the cavity, and thermal field fluctuations have to be minimized as the Fock states of the em field are fragile and extremely difficult to generate.

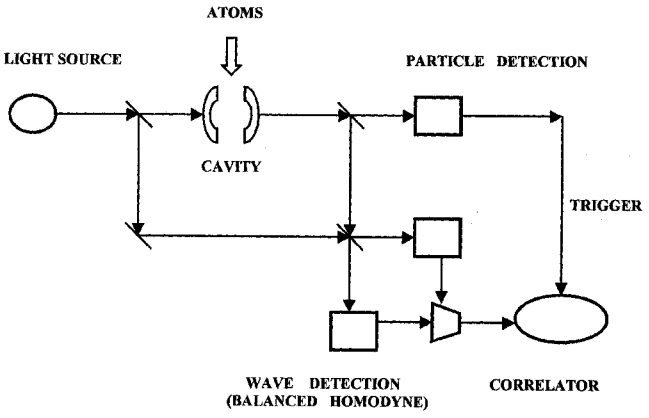

Figure 22. Schematic of the experiment used to measure wave–particle correlations for cavity QED light sources. The apparatus consists of a particle detection unit as well as a wave detection unit in terms of a balanced homodyne detection system.

We first discuss the trapping state of the em field[50,51]. The trapping states which peak at a single photon occupation number are features of the dynamical evolution of micromaser field, where the field is quantized in the micromaser cavity. The atom–field dynamics is governed by the JCM[3,23]. The trapping states are observed in micromaser cavity when it satisfies the condition

$$gt_{\text{int}}\sqrt{n_c+1} = m\pi, \tag{39}$$

where g is the atom–field coupling parameter, t_{int} is the time for which the incoming atoms interact with the field of cavity having n_c photons and atoms are undergoing exactly m Rabi oscillations. Here $m = 1, 2, 3...$, etc. represents the first, second, third..., etc. 'trapping states', respectively of the micromaser cavity field satisfying the above conditions (eq. 39). When a trapping state is realized by choosing proper parameters in eq. (39), the photon number distribution has got a cut-off at $n = n_c$ (see Figure 23) and hence the trapping state photon number distribution has an upper-bound photon number n_c. In order to observe trapping states in the cavity QED experiment (micromaser), the lifetime of the atomic state should be large and the cavity damping factor should be small (cavity with large Q value is preferable). In order to reduce thermal fluctuations, the cavity temperature should be as low as possible. The velocity distribution of the atomic beam should be very sharp and the atomic flux must be controlled in such a manner that the multiatom effects in the cavity experiments can be excluded. The experiment reported by the Munich group[45] has used a superconducting cavity with $Q = 1.5 \times 10^{10}$, $T = 300$ mK pumped by excited ^{85}Rb atoms (in state $63p_{3/2}$ with the frequency-doubled dye laser). The micromaser Rydberg transition used here is $63p_{3/2} \rightarrow 61d_{5/2}$ at frequency 21.5 GHz. In this experiment, the field variance of the micromaser cavity is measured using the statistics of the outcoming atoms. A trapping state shows ideal sub-Poissonian statistics (variance < 1) (Figure 24). Consequently, when the trapping state is realized by using proper interaction time, the atomic statistics is also sub-Poissonian. The Fano–Mandel parameter is equal to 0 for the Poissonian statistics and it is less (greater) than 0 for sub (super)-Poissonian statistics. Their methodology to analyse data is based on two different techniques. The first one is based on the atomic inversion measurement and the

second is a statistical approach based on the time spacing of the emerging ground state atoms.

The dips observed in inversion correspond to trapped states which correspond to reduced fluctuations in the atomic statistics. This is because at the photon number position of the trapping state, the cavity field builds up until it satisfies the conditions in eq. (39). So once the micromaser cavity field has achieved its trapping state, it will remains there whatsoever may be the pump rate. This is manifested as a dip in the atomic inversion[45]. The trapping state so generated under steady state represents a Fock state within a certain situation, as we will discuss subsequently. The method employed by the Munich group for generating Fock state in the cavity is based on entanglement between the atom and the field, and state reduction[52]. When the atom leaves the cavity the wave function of the entangled system is given according to Jaynes–Cummings dynamics

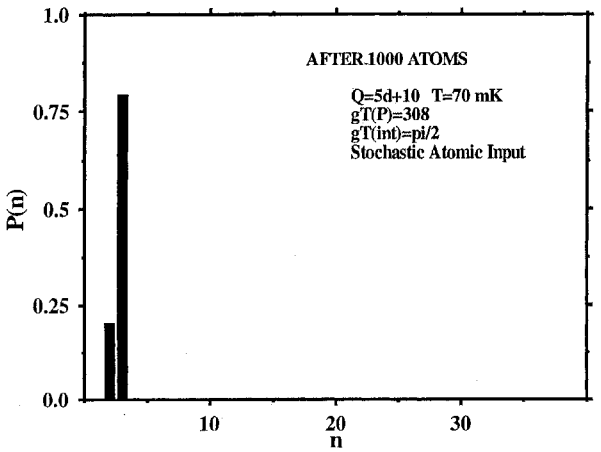

Figure 23. Trapping state dynamics observed for $N = 1000$ atoms, $gt_{int} = \pi/2$, $Q = 5 \times 10^{10}$, $T = 70$ mK, $gT_P = 308$. Stochastic atomic input has been used (see ref. 51 for details). The cut-off in photon number can be seen at $n = n_c = 3$ for the value selected here for the interaction time.

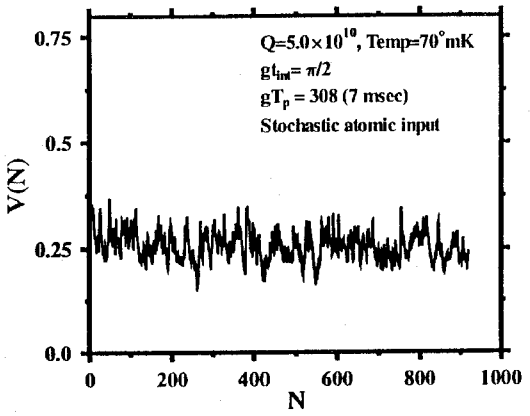

Figure 24. Variance as a function of number of atoms inside the cavity for the trapping state dynamics for the same parameters as in Figure 23. Clearly, we observe sub-Poissonian statistics.

$$|\psi(t)\rangle = \cos(\Theta)|e\rangle|n\rangle - \sin(\Theta)|g\rangle|n+1\rangle. \quad (40)$$

A simple meaning of the above wavefunction (in which Θ is a phase) is as follows: when the atom is in the excited (ground) state $|e\rangle(|g\rangle)$, the cavity field is in the Fock state $|n\rangle$ $(|n+1\rangle)$. So, state-selective photoionization measurement of the atomic state will reduce the field state to either one of the Fock states $|n\rangle$ or $|n+1\rangle$, depending upon whether the atom is detected in the excited state or in the ground state. Suppose the atoms are detected in their excited state, then the field will reduce to the $|n\rangle$ state. Hence determination of the state of outgoing atoms leads to a Fock state in the cavity. This method of production of the Fock state is called method of state reduction and it is independent of the cavity interaction time. The Monte Carlo simulation for this method is also presented elsewhere (see also Figure 18). The experimental conditions used in the Fock-state generation are quite similar to those used for detecting the trapped states. The Q factor of the cavity used here is 3.4×10^9 (corresponding to photon lifetime of 25 ms). In this experiment pulsed excitation of the atom has been used, so that the number of atoms passing through the cavity is predetermined. To verify whether the Fock state has been produced in the cavity, the pump-probe technique is utilized. With pump atoms, the cavity is producing a definite quantum state as the atoms are projected into or detected in the definite state. For verification of projection of the cavity field state in the proper quantum state, probe atoms are introduced into the cavity and the phase of the Rabi cycle of the emerging probe atom is measured to confirm the quantum state of the cavity. With this methodology they have demonstrated the preparation of the Fock state up to $n = 2$ in the microwave cavity. As mentioned earlier the 'trapping state' occurs at a definite interaction time; hence when the Fock state preparation experiment meets the condition of the 'trapping state' interaction time, the cavity field is identical to what is observed in steady-state conditions and the probe atom will undergo integral number of Rabi oscillations.

Concluding remarks

In conclusion, the fundamental model of a fermion–boson interaction has been exploited to great lengths both theoretically and experimentally, to study several basic aspects of quantum mechanics. New situations can be envisaged as the experimental techniques become progressively better. These experiments have strong influence on the upcoming technology of quantum information/computation. Current experiments are directed towards trapping and localization of atoms inside small cavities. This is being pursued by employing novel forces in cavity QED at the single-photon level,

and by utilizing dipole force traps within the cavity mode. To provide some kind of classical pondermotive potential for trapping an atom 'indefinitely', a new kind of trap called FORT (far-off resonance trap) is being utilized. There is intense thrust to investigate algorithms for continuous quantum variables besides quantum information processing within the internal states of the atoms with photons serving as qubits. A genuine quantum teleportation for the quadrature amplitude of light has been demonstrated[53]. Experiments for super-dense quantum coding are under progress. Hopefully, in the near future, with the progress in cavity QED experiments, it may be possible to teleport the center-of-mass wave function for atoms trapped in optical cavities[54].

1. Joshi, A. and Lawande, S. V., *Curr. Sci.*, 2002, **82**, 816–837.
2. Dirac, P. A. M., *Proc. R. Soc. London*, 1927, **A114**, 243; Feynman, R. P., *Phys. Rev.*, 1949, **76**, 749, 769; Bethe, H. A. and Salpeter, E. E., *Quantum Mechanics of One and Two-electron Systems*, Plenum, New York, 1977; Haroche, S., *Phys. World*, March 1991, p. 13.
3. Jaynes, E. T. and Cummings, F. W., *Proc. IEEE*, 1963, **51**, 89; Shore, B. W. and Knight, P. L., *J. Mod. Opt.*, 1993, **40**, 137.
4. Cummings, F. W., *Phys. Rev.*, 1965, **140**, 1051; *Frontiers in Quantum Optics* (eds Pike, E. R. and Sarkar, S.), Adam Higler, Bristol, 1986, p. 485.
5. Yoo, H.-I. and Eberly, J. H., *Phys. Rep.*, 1985, **118**, 239.
6. Knight, P. L. and Radmore, P. M., *Phys. Rev.*, 1982, **A26**, 676; *Phys. Lett.*, 1982, **90A**, 342; Joshi, A. and Lawande, S. V., *Phys. Rev.*, 1993, **A48**, 2276; *Phys. Lett.*, 1994, **A184**, 390; *Phys. Rev.*, 1994, **A50**, 1692; *J. Mod. Opt.*, 1995, **42**, 2561; *Phys. Rev.*, 1995, **A52**, 619; *J. Mod. Opt.*, 1987, **34**, 1421; 1989, **36**, 215; 1989, **36**, 557; *Opt. Commun.*, 1989, **69**, 369; 1989, **70**, 21; 1990, **75**, 189; *J. Mod. Opt.*, 1991, **38**, 1137, 1407.
7. Rempe, G., Walther, H. and Klien, N., *Phys. Rev. Lett.*, 1987, **58**, 353.
8. Meschede, D., Walther, H. and Muller, G., *ibid*, 1985, **54**, 551.
9. Filipowicz, P., Javanainen, J. and Meystre, P., *J. Opt. Soc. Am.*, 1980, **B2**, 908.
10. Brune, M., Raimond, J. M. and Haroche, S., *Phys. Rev.*, 1987, **A35**, 154.
11. Heinzen, D. and Feld, M. S., *Phys. Rev. Lett.*, 1987, **59**, 2623; Raizen, M. G., Thompson, R. J., Brecha, R. J., Kimble, H. J. and Carmichael, H. J., *ibid*, 1989, **63**, 240; Zhu, Y., Gauthier, D. J., Morrin, S. E., Wu, Q., Carmichael, H. J. and Mossberg, T. W., *ibid*, 1990, **64**, 2499; Haroche, S., Brune, M. and Raimond, J. M., AIP Conference Proceedings 233, *Atomic Physics 12* (eds Zorn, J. C. and Lewis, R. R.), 1991, 204; Joshi, A., *Phys. Lett.*, 2001, **A290**, 23.
12. Haroche, S., *New Trends in Atomic Physics* (eds Grynberg, G. and Stora, R.), North Holland, Amsterdam, 1984; Haroche, S. and Raimond, J. M., in *Advances in Atomic and Molecular Physics* (eds Bates and Bederson), 1984, vol. 20, p. 347.
13. Agarwal, G. S., *Phys. Rev. Lett.*, 1984, **53**, 1732; *J. Opt. Soc. Am.*, 1985, **B2**, 480; Joshi, A. and Lawande, S. V., *J. Mod. Opt.*, 1993, **40**, 1035.
14. Bohm, D., *Quantum Theory*, Prentice Hall, Englewood Cliffs, 1951.
15. Wootters, W. and Zurek, W., *Phys. Rev.*, 1979, **D19**, 473; Wheeler, J. A. and Zurek, W. H., *Quantum Theory and Measurements*, Princeton University Press, 1983, Chap. 1.
16. Englert, B.-G., Schwinger, J. and Scully, M. O., *Found. Phys.*, 1988, **18**, 1045; Schwinger, J., Scully, M. O. and Englert, B.-G., *Z. Phys.*, 1988, **D10**, 135; Scully, M. O., Englert, B.-G. and Schwinger, J., *Phys. Rev.*, 1989, **A40**, 1775; Scully, M. O. and Walther, H., *ibid*, 1989, **A39**, 5229; Rempe, G., Scully, M. O. and Walther, H., AIP Conference Proceedings 233, Atomic Physics 12 (eds Zorn, J. C. and Lewis, R. R.), 1991, p. 219.
17. Haroche, S., *High Resolution Laser Spectroscopy*, Springer, Berlin, 1976; Chow, W. W., Scully, M. O. and Stoner, J. O., *Phys. Rev.*, 1975, **A11**, 1380.
18. Feynman, R., Leighton, R. and Sands, M., *The Feynman Lectures on Physics*, Addison-Wesley, Reading, MA, 1965, vol. 3, p. 5.
19. Scully, M. O., Englert, B.-G. and Walther, H., *Nature*, 1991, **351**, 111; *Sci. Am.*, December 1994, 56; Bertet, P. *et al.*, *Nature*, 2001, **411**, 166.
20. Raithel, G., Wagner, C., Walther, H., Narducci, L. M. and Scully, M. O., in *Cavity Quantum Electrodynamics* (ed. Berman, P. R.), Academic Press, 1994.
21. Herzog, T. J., Kwiat, P. G., Weinfurter, H. and Zeilinger, A., *Phys. Rev. Lett.*, 1995, **75**, 3034.
22. Chapman, M. S., Hammond, T. D., Lenef, A., Schmiedmayer, J., Rubenstein, R. A., Smith, E. and Pritchard, D. E., *Phys. Rev. Lett.*, 1995, **75**, 3783 and references therein; For another interesting experiment, see for example, Kokorowski, D. E., Cronin, A. D., Roberts, T. D. and Pritchard, D. E., arXiv: quant-ph/0009044 v2, 2001.
23. Joshi, A., Ph D thesis, University of Bombay, 1991 (unpublished); Joshi, A. and Lawande, S. V., *Opt. Eng.*, 1994, **33**, 1964; *Phys. Rev.*, 1990, **A42**, 1752; 1991, **A44**, 2135; 1992, **A45**, 5056; 1993, **A48**, 2276; 1998, **A58**, 4662; 2000, **A62**, 043812; Dung, H. T., Joshi, A. and Knoll, L., *J. Mod. Opt.*, 1998, **45**, 1067; Joshi, A. and Dung, H. T., *Mod. Phys. Lett.*, 1999, **B13**, 143; for other related work in the same area, see, Joshi, A. *et al.*, *Phys. Rev.*, 1990, **A42**, 4436; 1992, **A46**, 5906.
24. Purcell, E. M., *Phys. Rev.*, 1946, **69**, 681.
25. Drexhage, K. H., *Progress in Optics* (ed. Wolf, E.), North Holland, New York, 1974, vol. 12.
26. Hinds, E. A., in *Cavity QED* (ed. Berman, P. R.), Associated Press, New York, 1994.
27. Casimir, H. B. G. and Podler, D., *Phys. Rev.*, 1948, **73**, 360; Casimir, H. B. G., *Proc. K. Ned. Akad. Wet.*, 1948, **51**, 793.
28. Goy, P., Raymond, J. M., Gross, M. and Haroche, S., *Phys. Rev. Lett.*, 1983, **50**, 1903.
29. Kleppner, D., *ibid*, 1981, **47**, 233.
30. Hulet, R. G., Hilfer, E. S. and Kleppner, D., *ibid*, 1985, **55**, 2137.
31. Jhe, W., Anderson, A., Hinds, E. A., Meschede, D., Moi, L. and Haroche, S., *ibid*, 1987, **58**, 666.
32. Berry, M. V., *Proc. R. Soc. London*, 1984, **A392**, 45; Simon, B., *Phys. Rev. Lett.*, 1983, **51**, 2167.
33. Aharonov, Y. and Anandan, J., *Phys. Rev. Lett.*, 1987, **58**, 1595.
34. Pancharatnam, J., *Proc. Indian Acad. Sci.*, 1956, **A44**, 217.
35. Bhandari, R. and Samuel, J., *Phys. Rev. Lett.*, 1988, **60**, 1210.
36. Lawande, Q. V., Lawande, S. V. and Joshi, A., *Phys. Lett.*, 1999, **A251**, 164; Joshi, A., Pati, A. K. and Banerjee, A., *Phys. Rev.*, 1994, **A49**, 5131; Pati, A. K. and Joshi, A., *ibid*, 1993, **A47**, 98; Pati, A. K. and Joshi, A., *Europhys. Lett.*, 1993, **21**, 723; Gantsog, Ts., Joshi, A. and Tanas, R., *Quantum Opt.*, 1994, **6**, 517; *Quantum Semiclassical Opt.*, 1996, **8**, 445; Vaccaro, J. A. and Joshi, A., *Phys. Lett.*, 1998, **243**, 13; Joshi, A. *et al.*, *Acta Phys. Slovaca*, 1998, **48**, 23.
37. Brune, M. *et al.*, *Phys. Rev. Lett.*, 1996, **76**, 1800; **77**, 4887; Ekert, A. and Jozsa, R., *Rev. Mod. Phys.*, 1996, **68**, 733.
38. Garrison, J. C. and Chiao, R. Y., *Phys. Rev. Lett.*, 1988, **60**, 165; Suter, D., Mueller, K. T. and Pines, A., *ibid*, 1988, **60**, 1218.
39. Shapiro, J. H. and Shepard, S. R., *Phys. Rev.*, 1991, **43**, 3795.

40. Haroche, S., *Fundamental Systems in Quantum Optics* (eds Dalibard, J., Raymond, J. M. and Zinn-Justin, J.), Elsevier, 1994; Haroche, S. and Raimond, J. M., in *Cavity Quantum Electrodynamics* (ed. Berman, P.), 1994, p. 123; see also ref. (12); Haroche, S., Brune, M. and Raimond, J. M., AIP Conference Proceedings, 275, *Atomic Physics 13* (eds Walther, H., Hansch, T. W. and Neizert, B.), 1992, p. 261 and references therein; Raimond, J. M., Brune, M. and Haroche, S., *Rev. Mod. Phys.*, 2001, **73**, 565; Brune, M. *et al.*, *Phys. Rev.*, 1992, **A45**, 5193.
41. Nogues, G., Rauschenbeutel, A., Osnagchi, S., Brune, M., Raimond, J. M. and Haroche, S., *Nature*, 1999, **400**, 239.
42. Rauschenbeutel, A. *et al.* (to be published).
43. Meekhof, D. M., Monroe, C., King, B. E., Itano, W. M. and Wineland, D. J., *Phys. Rev. Lett.*, 1996, **76**, 1796; Monroe, C., Meekhof, D. M., King, B. E., Jefferts, S. R., Itano, W. M., Wineland, D. J. and Gould, P., *ibid*, 1995, **75**, 4011; Jefferts, S. R., Monroe, C., Bell, E. W. and Wineland, D. J., *Phys. Rev.*, 1995, **A51**, 3112; Monroe, C., Meekhof, D. M., King, B. E., Jefferts, S. R. and Wineland, D. J., *Science*, 1996, **272**, 1131.
44. Yeazell, J. A. and Stroud Jr. C. R., *Phys. Rev. Lett.*, 1988 **60**, 1494; A Ten Wolde *et al.*, *ibid*, 1988, **61**, 2099.
45. Varcoe, B. T. H., Brattke, S., Weidlinger, M. and Walther, H., *Nature*, 2000, **403**, 743; Weidlinger, M., Varcoe, B. T. H., Heerlein, R. and Walther, H., *Phys. Rev. Lett.*, 1999, **82**, 3795.
46. deMatos Filho, R. L. and Vogel, W., *Phys. Rev.*, 1996, **A54**, 4560 and references therein; Man'ko, V. I., Marmo, G., Sudershan, E. C. G. and Zaccaria, F., *Phys. Scr.*, 1997, **55**, 528; Vogel, W. and deMatos Filho, R. L., *Phys. Rev.*, 1995, **A52**, 4214; Joshi, A., *J. Opt.*, 2001, **B3**, 124.
47. Mabuchi, H., Turchette, Q. A., Chapman, M. S. and Kimble, H. J., *Opt. Lett.*, 1996, **21**, 1393; Hood, C. J., Lynn, T. W., Doherty, A. C., Perkins, A. S. and Kimble, H. J., *Science*, 2000, **287**, 1447; Ye, J., Vernooy, D. W. and Kimble, H, J., quant-ph/9908007v1.
48. Pinkse, P. W. H., Fischer, T., Maunz, P. and Rempe, G., *Nature*, 2000, **404**, 365.
49. Carmichael, H. J., Quant-ph/0104073; Foster, G. T., Orozco, L. A., Castro-Beltran, C. M. and Carmichael, H. J., *Phys. Rev. Lett.*, 2000, **85**, 3149; Carmichael, H. J., Castro-Beltran, C. M., Foster, G. T. and Orozco, L. A., *ibid*, 1855.
50. Meystre, P., Rempe, G. and Walther, H., *Opt. Lett.*, 1988, **13**, 1078; Raithel, G. *et al.*, in *Cavity Quantum Electrodynamics* (ed. Berman, P. R.), Academic Press, New York, 1994.
51. Joshi, A., Bullough, R. K. and Thompson, B. V., *J. Mod. Opt.*, 1996, **43**, 971; *SPIE Proceedings* (ed. Bagayev, S. N.), 1996, vol. 2799; Bullough, R. K., Joshi, A. and Thompson, B. V., in *Notions and Perspective of Nonlinear Optics*, 1996, vol. 3, 10; Joshi, A., *Laser Phys.*, 1997, **47**, 68.
52. Krause, J., Scully, M. O. and Walther, H., *Phys. Rev.*, 1987, **A36**, 4547.
53. Furusawa, A., Sorensen, J. L., Braunstein, S. L., Fuchs, C. A., Kimble, H. J. and Polzik, E. S., *Science*, 1998, **282**, 706.
54. Parkins, A. S. and Kimble, H. J., quantum-ph/9904062.

ACKNOWLEDGEMENTS. We thank Prof. Howard Carmichael, Prof. H. J. Kimble, Prof. Surendra Singh, Prof. H. Walther and Dr John Vaccaro for many helpful discussions. We also thank our colleagues, Prof. R. K. Bullough, Prof. G. S. Agarwal, Dr Q. V. Lawande and Dr R. D'Souza for their support. SVL thanks CSIR for generous financial support.

Received 27 July 2001; revised accepted 14 February 2002